

Baryon Junction and String Interactions: Part II

Xuzixiang Lou¹ and Siwei Zhong^{1,2}

¹*Simons Center for Geometry and Physics, Stony Brook University,
Stony Brook, NY 11794, USA*

²*C. N. Yang Institute for Theoretical Physics, Stony Brook University,
Stony Brook, NY 11794, USA*

E-mail: xuzixiang.lou@stonybrook.edu, siwei.zhong@stonybrook.edu

ABSTRACT: We study junctions between confining strings, extending the analysis of [1]. These junctions arise in Yang-Mills theories, and we focus on their universal low-energy dynamics. Using open-closed duality, we map junctions with nonlinear corrections to the s -wave scattering amplitudes between confining string loops. In $(3 + 1)$ dimensions, we uncover an accidental \mathbb{Z}_2 symmetry. This symmetry implies novel selection rules for loop scattering amplitudes and is broken by the junction mass at subleading order. We determine the total mass of baryons up to order (baryon size)⁻³, providing new, testable predictions for lattice simulations.

Contents

1	Introduction and summary	1
2	Review of the effective string theory	3
2.1	Open string boundary conditions	5
2.2	Open-closed duality	6
2.3	Baryon junction condition	8
3	Open-closed duality of baryon junctions	11
3.1	Partition function of the probe baryon	12
3.2	S -wave scattering	14
3.3	An accidental \mathbb{Z}_2 symmetry	16
4	Nonlinear corrections	20
4.1	Regularized corrections to the partition function	20
4.2	Saddle-point approximation	22
5	Ground state energies of probe baryons	24
A	Modular functions	27
B	Probe baryons at rational points	27
C	Green's functions on a cylinder	30
C.1	Wick contraction	31
C.2	Zeta-function regularization	33

1 Introduction and summary

Confinement is a fascinating phenomenon at the heart of modern physics. Since the discovery of asymptotic freedom [2, 3], sustained efforts have been devoted to understanding the mechanism in the Standard Model that confines color quarks inside hadrons. Evidence from lattice simulations [4, 5] and simplified theoretical models [6, 7] indicates that the chromoelectric flux between quarks forms string-like excitations with nonzero tension, known as the QCD flux tubes. This phenomenon also occurs in type-II superconductors, where magnetic monopoles are confined by the Abrikosov vortices [8]. Other models exhibiting similar confining strings include $(1 + 1)$ -dimensional QED [9], $(2 + 1)$ -dimensional $U(1)$ gauge theory with monopole-instantons [10], $(2 + 1)$ -dimensional \mathbb{Z}_2 gauge theory [11, 12], and Seiberg–Witten theory with softly broken supersymmetry [13]. When local excitations

are fully gapped, these string-like excitations are stable against breaking and can only end on probe particles or other strings.

The dynamics of the confining strings are elusive at first sight, since the underlying field theory is often strongly coupled at long distances (e.g., $(3 + 1)$ -dimensional QCD). For sufficiently long strings, however, it was shown under mild assumptions that their low-energy dynamics are uniquely determined by the Nambu–Goto action [14–17]. This action describes the shape fluctuations of a string with tension l_s^{-2} and is given by [18, 19]

$$S_{\text{NG}} = -l_s^{-2} \int dt d\sigma \sqrt{-\det(\partial_\alpha X^\mu \partial_\beta X_\mu)} , \quad (1.1)$$

where $X^\mu(t, \sigma)$ is the embedding of the string worldsheet in $(d + 1)$ -dimensional spacetime. For short strings, quantization of the Nambu–Goto action spoils Lorentz invariance outside the critical dimension $d = 25$. Nevertheless, the action (1.1) defines a consistent effective theory for fluctuations around long-string backgrounds in arbitrary dimension d . It thereby follows that long confining strings in different theories share common properties that are controlled by the string tension l_s^{-2} at low energies.

The junctions are important structures that connect multiple confining strings. They are directly observed inside baryonic states in lattice simulations of $(3 + 1)$ -dimensional QCD [20–23], and are commonly referred to as baryon junctions. When the strings are associated with 1-form symmetries, these junctions exist provided they satisfy the fusion rules. For example, multiple Nielsen–Olesen strings can meet at a junction when their magnetic charges sum to zero. For a partial list of early and recent studies on the baryon junctions, see, e.g., [1, 24–32].

Do baryon junctions also exhibit universal low-energy dynamics? In our previous work [1] and this paper, we address this question in the effective field theory framework. We focus on trivalent junctions and argue that their low-energy dynamics are controlled by the junction mass M . In particular, we determine the ground state energy of a probe baryon, consisting of three identical strings of length L meeting at a junction, up to order L^{-3} :

$$E_{\text{GS}} = \frac{3L}{l_s^2} + M - \frac{(d-2)\pi}{16L} - \frac{(d+2)\pi M l_s^2}{144L^2} + \boxed{\frac{(d+6)\pi M^2 l_s^2}{432L^3} - \frac{(d-2)^2 \pi^2 l_s^2}{1536L^3}} + O(L^{-4}) , \quad (1.2)$$

where the boxed L^{-3} term provides a new prediction for lattice simulations. We note that the expansion coefficients, up to high orders, are fixed by the junction mass M and the string tension l_s^{-2} .

The simple low-energy dynamics of the baryon junction have deep implications for the interactions between long closed strings (i.e., glueball-like excitations). These two seemingly different subjects are related by the *open-closed duality* [33, 34], which we analyze explicitly in this work. Crucially, we map the baryon junction to local interactions that govern the s -wave scattering of confining string loops. For strings wrapped on a circle of circumference $2\pi R$, we find that the scattering amplitudes pick up the overall factor

$$e^{-2\pi R M} . \quad (1.3)$$

Consequently, interactions between large loops are exponentially suppressed when the junction mass is positive. From consistency conditions, we explicitly determine the interaction vertices at leading orders in the R^{-1} expansion.

From short to long distances, a natural question is what physical scale sets the junction mass M in the effective field theory. We generally expect that $M \sim l_s^{-1}$ and is set by the mass gap of the underlying quantum field theory. In the large N expansion, M scales as the total energy of attached strings¹, and the junction becomes parametrically heavy [27, 29, 35]. In this paper, we identify a novel \mathbb{Z}_2 symmetry for strings in $(3+1)$ -dimensional spacetime that is broken by the junction mass M at subleading order. See equation (3.25). It would be intriguing to understand whether this \mathbb{Z}_2 symmetry can be realized at short distances and thereby requires $M = 0$.

The rest of the paper is organized as follows. Section 2 provides a brief review of effective string theory. In Section 2.3, we summarize the effective description of the baryon junction introduced in [1]. We establish the open-closed duality of the baryon junction in Section 3. In particular, the worldsheet formulation of the novel \mathbb{Z}_2 symmetry and its implications in the closed channel are discussed in Section 3.3. Section 4 extends the open-closed duality to higher orders, incorporating nonlinear corrections from the confining strings and the baryon junction. Finally, we discuss quantum corrections to the ground state energies (i.e., masses) of probe baryons in Section 5 and Appendix B.

We close by commenting on the relation to our previous work. In [1], the open-closed duality of baryon junctions was analyzed for a special string-junction configuration with linear quantum fluctuations. In this paper, we extend the picture to general configurations as in figure 1 and also include higher-order nonlinear corrections. Some results from [1] are reproduced and generalized in equations (3.23), (4.10) and (5.6).

2 Review of the effective string theory

We first review the effective field theory of long confining strings in $(d+1)$ -dimensional spacetime. See also [1, 14–17, 36–50] for a necessarily incomplete selection of references.

From a modern perspective, an infinitely long confining string is a vacuum of the underlying UV theory that spontaneously breaks the Poincaré symmetry $ISO(d, 1)$ down to $ISO(1, 1) \times SO(d-1)$. The group $ISO(1, 1)$ denotes the residual Poincaré symmetry along the string direction, whereas $SO(d-1)$ is the transverse rotation group. This symmetry-breaking pattern gives rise to exactly $(d-1)$ Nambu–Goldstone Bosons (NGBs) [51] that describe transverse fluctuations of the string. In the rest of this paper, we assume that there are no other degrees of freedom in the low-energy effective theory of the string other than these NGBs.² This assumption applies to a wide class of gapped confining gauge theories, including the pure $SU(N)$ Yang–Mills theory in $(3+1)$ and $(2+1)$ dimensions [55–57].

¹In the 't Hooft limit, the junction mass is of order N for D5-brane realizations and order N^2 for NS5-brane realizations.

²In supersymmetric gauge theories, there are also fermionic modes localized on the BPS confining strings [52–54]. These cases are beyond the scope of this paper.

The effective action of NGBs localized on the confining string is strongly constrained by the nonlinearly realized Poincaré symmetry and by worldsheet diffeomorphism invariance. The leading terms in the low-energy expansion of the effective string theory are dominated by the Nambu–Goto action (1.1), such that

$$S_{\text{string}} = - \int dt d\sigma \sqrt{-\det(\partial_\alpha X^\mu \partial_\beta X_\mu)} [l_s^{-2} + O(\partial^6)] . \quad (2.1)$$

The leading higher-derivative corrections in the action (2.1) include the Polyakov–Kleinert rigidity term [58, 59] at $O(\partial^6)$. Taking advantage of the diffeomorphism invariance, we can choose the static gauge of the worldsheet embedding $X_\mu(t, \sigma)$ as

$$X_0 = t , \quad X_1 = \sigma , \quad \text{and} \quad X_i = l_s x_i(t, \sigma) \text{ for } 2 \leq i \leq d . \quad (2.2)$$

The effective string action (2.1) under the ghost-free gauge (2.2) takes the expansion form

$$S_{\text{string}} = \int dt d\sigma \left[-\frac{1}{l_s^2} + \frac{1}{2} ((\partial_t x_i)^2 - (\partial_\sigma x_i)^2) + \frac{l_s^2}{8} (\partial_t x_i - \partial_\sigma x_i)^2 (\partial_t x_{i'} + \partial_\sigma x_{i'})^2 + O(\partial^6) \right] , \quad (2.3)$$

where both the $O(\partial^2)$ quadratic term and the $O(\partial^4)$ quartic term follow from the Nambu–Goto action.

We now specify our EFT order counting convention as follows: terms in the confining string worldsheet action are of order n if they scale as $O(\partial^{n+2})$; terms supported on the 1-dimensional submanifold of the worldsheet are of order n if they scale as $O(\partial^{n+1})$. In this convention, classical contributions to the path-integral are denoted by terms with negative orders, whereas the leading quantum corrections start at order 0. For example, the three terms in the action (2.3) are of orders -2 , 0 , and 2 , respectively. The order 0 quadratic term in (2.3) is simply the kinetic term of free worldsheet bosons, whereas the order 2 quartic term corresponds to a $T\bar{T}$ -deformation of the free theory [60–62]. Notably, the effective string action (2.3) is completely determined by the classical string tension l_s^{-2} up to order 3.

The action (2.3) can be used to compute the spectrum of a long, closed confining string with high precision. We consider a string that wraps along the periodic X_1 -direction of circumference $2\pi R$, such that in the static gauge (2.2) we have $\sigma \sim \sigma + 2\pi R$. The energy of a generic closed string state takes the following form [14, 17, 39, 63]

$$E_a^{\text{closed}} = \frac{2\pi R}{l_s^2} + \frac{2}{R} \left(n_a - \frac{d-1}{24} \right) - \frac{l_s^2}{\pi R^3} \left(n_a - \frac{d-1}{24} \right)^2 + O(R^{-5}) , \quad (2.4)$$

where the subscript a (and similarly b and c below) labels weakly coupled multi-particle states on the closed string. In equation (2.4), n_a denotes the average of the left- and right-moving excitation levels, following from the order 0 free kinetic term in the action (2.3)³. For states with vanishing momentum along the X_1 -direction, we have $n_a \in \mathbb{N}$.

³In the free theory approximation of (2.4), the worldsheet Hamiltonian of the closed string reads

$$H_{\text{free}} = \sum_{i=2}^d \sum_{n \in \mathbb{N}^+} \frac{n}{R} \left((\alpha_{\text{L},n}^i)^\dagger \alpha_{\text{L},n}^i + (\alpha_{\text{R},n}^i)^\dagger \alpha_{\text{R},n}^i \right) - \frac{d-1}{12R} ,$$

We note from (2.4) that there exists a large degeneracy between closed string excited states at the precision of $O(R^{-3})$, which is a consequence of the Poincaré symmetry and the integrability of the quartic deformation in (2.3). In the following sections, we will be interested in states that transform in the scalar representation of the transverse rotation group $SO(d-1)$ and carry zero longitudinal momentum. The two lowest-lying states satisfying these conditions are the ground state $\mathbf{0}$ (with $n_{\mathbf{0}} = 0$) and an excited state $\mathbf{1}$ (with $n_{\mathbf{1}} = 1$), while states with excitation levels $n_a \geq 2$ are degenerate.

2.1 Open string boundary conditions

In this subsection, we review the Dirichlet and the Neumann boundary effective theories of open confining strings. See, e.g., [14, 15, 40] for a systematic and detailed analysis.

Let us consider a semi-infinite string with longitudinal coordinate $X_1 = \sigma \geq 0$, whose worldsheet action is given by (2.3). The variational principle of the order 0 kinetic term in (2.3) leads to two canonical choices of boundary conditions at $\sigma = 0$, namely Dirichlet and Neumann. The Dirichlet boundary condition that preserves $SO(d-1)$ rotation symmetry reads

$$\text{Dirichlet : } \quad \partial_t x_i = 0, \quad \text{for } 2 \leq i \leq d. \quad (2.5)$$

It is also convenient to set the NGBs $x_i = 0$ at the Dirichlet boundary $\sigma = 0$. Higher-order corrections of the Dirichlet boundary are constrained by Poincaré symmetry, and the leading boundary deformation takes the following form:

$$S_{\text{Dirichlet}} = \int_{\sigma=0} dt [-m_{\text{D}} + \kappa_{\text{D}}(\partial_t \partial_\sigma x_i)^2 + O(\partial^6)]. \quad (2.6)$$

The m_{D} term in (2.6) is of order -1 according to our EFT counting convention, whereas the κ_{D} term is of order 3. The constant m_{D} simply shifts the zero-point energy associated with the Dirichlet boundary. In lattice simulations, m_{D} represents the scheme-dependent mass of the static quarks. For convenience, we set $m_{\text{D}} = 0$ throughout this paper, i.e., we subtract the quark mass contributions.

On the other hand, the $SO(d-1)$ symmetric Neumann boundary condition reads

$$\text{Neumann : } \quad \partial_\sigma x_i = 0, \quad \text{for } 2 \leq i \leq d. \quad (2.7)$$

Similarly, we can consider higher-order corrections to the Neumann boundary condition that are compatible with the Poincaré symmetry. The leading deformations are as follows

$$\begin{aligned} S_{\text{Neumann}} &= \int_{\sigma=0} dt \left[-m_{\text{N}} \sqrt{-(\partial_t X_\mu)^2} + \kappa_{\text{N}} (\partial_t^2 x_i)^2 + O(\partial^6) \right] \\ &= \int_{\sigma=0} dt \left[-m_{\text{N}} + \frac{m_{\text{N}} l_s^2}{2} (\partial_t x_i)^2 - \frac{m_{\text{N}} l_s^4}{8} (\partial_t x_i)^4 + \kappa_{\text{N}} (\partial_t^2 x_i)^2 + O(\partial^6) \right]. \end{aligned} \quad (2.8)$$

The first term in (2.8) denotes the worldline length of the dynamical string endpoint, where the parameter m_{N} is interpreted as the endpoint mass. We note that both the order -1

where $\alpha_{\text{L},n}^i$ and $\alpha_{\text{R},n}^i$ are the n -th annihilation operator left- and right-moving oscillator modes, respectively. Eigenvalues of H_{free} take the form of $\frac{2}{R}(n_a - \frac{d-1}{24})$, as explained below equation (2.4).

and order 1 terms in (2.8) are fixed by the mass m_N , whereas at order 3 an additional parameter κ_N can be introduced. Unlike m_D in (2.6), m_N perturbs the spectrum associated with the Neumann boundary.

2.2 Open-closed duality

We now follow [14, 38, 40, 64] and discuss the duality that associates the open string spectrum with an effective theory of closed string fields. For simplicity, we consider a finite string extending from $X_1 = \sigma = 0$ to $X_1 = \sigma = L$, with the Dirichlet boundary condition (2.5) at both ends. This confining string configuration describes a probe meson.

The partition function of the finite open string, denoted by \mathcal{Z} , can be computed and interpreted in several equivalent ways. In the open channel, the partition function is given by the Boltzmann sum

$$\text{open channel : } \mathcal{Z} = \sum_{E_{\text{open}}} e^{-\beta E_{\text{open}}} , \quad (2.9)$$

where E_{open} denotes the energy eigenvalues of open string states defined on $0 \leq \sigma \leq L$, and β is the inverse temperature. The partition function can be obtained by Wick rotating $t \rightarrow -i\tau$ and compactifying $\tau \sim \tau + \beta$ in the path-integral of the effective string action (2.3). In particular, we take the circumference of the Euclidean time circle to be $\beta = 2\pi R$. The open string partition function takes the following form

$$\mathcal{Z} = \frac{e^{-2\pi RL/l_s^2}}{[\eta(q)]^{(d-1)}} \left[1 - \frac{(d-1)\pi l_s^2}{1152L^2} \ln q (2E_4(q) + (d-3)(E_2(q))^2) + O(\partial^3) \right] , \quad (2.10)$$

where the modular parameter $q \equiv \exp(-2\pi^2 R/L)$, $\eta(q)$ denotes the Dedekind eta function, and $E_2(q)$, $E_4(q)$ are the Eisenstein series (see Appendix A). In the expansion (2.10), terms that scale as $O(L^{-n_1} R^{-n_2})$ have been collectively denoted by $O(\partial^{n_1+n_2})$. We note that order n terms in the effective action give leading contributions to the partition function that scale as $O(\partial^n)$. For example, corrections to the string endpoints, parametrized by κ_D (2.6) at $\sigma = 0$ and $\sigma = L$, are grouped into $O(\partial^3)$ terms in the expansion (2.10).

In the closed channel, the partition function is interpreted as the two-point function of the Polyakov loop operators wrapped along the X_0 -direction. A wrapped Polyakov loop preserves the Lorentz symmetry in the d -dimensional space spanned by the coordinates $\vec{X} = (X_1, X_{2 \leq i \leq d})$, and it defines a scalar point operator $\Omega(\vec{X})$. In general, the reducible operator Ω admits a decomposition into massive particle fields in the gapped effective theory as follows:

$$\Omega(\vec{X}) = (\pi l_s^2)^{\frac{d-1}{4}} \sum_a v_a \sqrt{E_a^{\text{closed}}} \Phi_a(\vec{X}) , \quad (2.11)$$

where $v_a \in \mathbb{C}$ denote decomposition coefficients, and Φ_a are d -dimensional complex scalar fields with definite masses. In equation (2.11) (and similarly below), the summation runs over Dirichlet boundary states of a confining closed string with circumference $2\pi R$. These boundary states reduce to Ishibashi states in the free theory limit, and are perturbed by higher-order corrections in the action (2.3) and (2.6). These closed string states satisfy

the following properties: (i) they carry zero longitudinal momentum, as required by the Cardy condition [34]; and (ii) they transform in the scalar representation of the transverse rotation group $SO(d-1)$, which is preserved by the Dirichlet condition (2.5). As we noted previously, the two lowest-lying boundary states are the ground state $\mathbf{0}$ and the excited state $\mathbf{1}$. We have also chosen the normalization in the decomposition (2.11) such that the coefficients v_a are dimensionless.

We adopt the following effective action ansatz for the dynamics of the closed-string fields Φ_a in d -dimensional space:

$$S_{\text{loops}} = \int d^d \vec{X} \left[\frac{1}{2} \sum_a (|\partial_\nu \Phi_a|^2 + (E_a^{\text{closed}})^2 |\Phi_a|^2) + V(\Phi_a, \Phi_b, \dots) \right], \quad (2.12)$$

where $V(\Phi_a, \Phi_b, \dots)$ denotes interaction terms. The functional $V(\Phi_a, \Phi_b, \dots)$ is constrained by 1-form symmetries of the confining strings, whether IR emergent or UV exact. We will investigate the structure of $V(\Phi_a, \Phi_b, \dots)$ in Sections 3 and 4. Notably, the mass of the field Φ_a corresponding to the closed-string state a is given by (2.4). From a d -dimensional viewpoint, E_a^{closed} plays the role of the internal mass of a particle at rest.

Following the decomposition (2.11) and the effective action (2.12), we find that the closed channel partition function takes the form

$$\text{closed channel : } \mathcal{Z} = \langle \Omega^\dagger(\vec{X}) \Omega(\vec{X}') \rangle = \sum_a |v_a|^2 \frac{(E_a^{\text{closed}})^{\frac{d}{2}} l_s^{d-1}}{\sqrt{\pi} (2L)^{\frac{d-2}{2}}} K_{\frac{d-2}{2}}(E_a^{\text{closed}} L), \quad (2.13)$$

where $|\vec{X} - \vec{X}'| = L$, and $K_\alpha(x)$ denotes the modified Bessel function of the second type. In equation (2.13), we have used the tree-level propagator of massive particles in d -dimensional space and omitted possible loop corrections from the interaction terms. Such loop corrections are exponentially suppressed by the mass scale $O(E_a^{\text{closed}}) = O(R/l_s^2)$, and the partition function is therefore heavily dominated by the contribution in (2.13). With the dual modular parameter given by $\tilde{q} \equiv \exp(-2L/R)$, the partition function (2.13) admits the expansion

$$\mathcal{Z} = \left(\frac{\pi R}{L} \right)^{\frac{d-1}{2}} \frac{e^{-2\pi R L / l_s^2}}{\tilde{q}^{\frac{d-1}{24}}} \sum_a |v_a|^2 \tilde{q}^{n_a} \left[1 - \frac{(d-1)l_s^2}{2\pi R^2} \left(\frac{\ln \tilde{q}}{d-1} \left(n_a - \frac{d-1}{24} \right)^2 - \left(n_a - \frac{d-1}{24} \right) + \frac{d-3}{4 \ln \tilde{q}} \right) + O(\partial^3) \right]. \quad (2.14)$$

The open-closed duality identifies the partition functions evaluated in the open channel (2.9) and in the closed channel (2.13). Consequently, each term in the expansion (2.10) is matched to the corresponding term in (2.14) by a modular transformation. This leads to strong constraints on the decomposition coefficients v_a . By locality, the coefficients $v_a = v_a(l_s, R, \kappa_D, \dots)$ are fixed solely by the local parameters of the Dirichlet boundaries, which are implemented by the Polyakov loops. From (2.9) and (2.14), we find that

$$\begin{aligned} v_{\mathbf{0}} &= 1 + \frac{(d-1)l_s^2}{48\pi R^2} + O(R^{-3}), \\ v_{\mathbf{1}} &= \sqrt{d-1} \left(1 + \frac{(d-25)l_s^2}{48\pi R^2} + O(R^{-3}) \right), \end{aligned} \quad (2.15)$$

to which we will return in Sections 3 and 4.

2.3 Baryon junction condition

In this subsection, we review the effective field theory of the trivalent baryon junctions introduced in [1]. We consider the confining string configurations as in figure 1, which describe probe baryons composed of three identical quarks. Our analysis applies, for example, to baryonic states in $SU(3N)$ pure Yang-Mills theories in $(2+1)$ and $(3+1)$ dimensions.

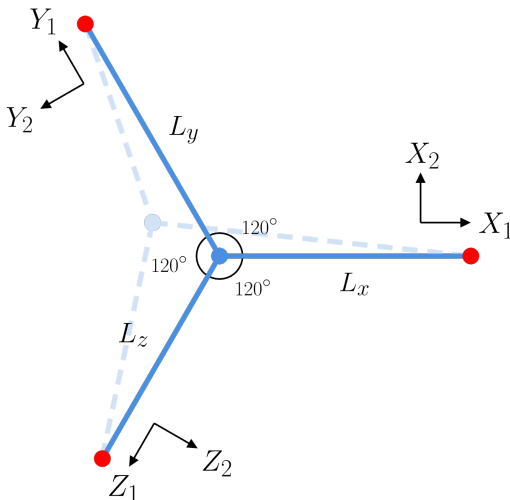


Figure 1: Confining strings in a probe baryon. The figure shows the spatial plane determined by the insertions of three static quarks (red points). The confining strings (blue lines) are tied at the dynamical baryon junction (blue point) and terminate on the quarks at their other ends.

Classically, the junction position in the d -dimensional space is determined by balancing the tensions l_s^{-2} of the three confining strings. It therefore coincides with the Fermat–Weber point of the triangle whose vertices are set by the quarks. Throughout this paper, we focus on baryon configurations where the Fermat–Weber point lies within the interior of the triangle. We leave the cases where the baryon junction overlaps with one of the quarks to future work.

We denote the coordinates of three strings by X_μ , Y_μ , and Z_μ , with their lengths L_x , L_y , and L_z . See also figure 1. In the static gauge (2.2), we take $X_1 = Y_1 = Z_1 = \sigma = 0$ to be the joint baryon junction where three strings are connected, while $X_1 = \sigma = L_x$, $Y_1 = \sigma = L_y$, and $Z_1 = \sigma = L_z$ are the string endpoints on the quarks. Furthermore, we use x_i , y_i , and z_i for the NGBs on the corresponding worldsheet. In our previous work [1], we argued that the effective action of the probe baryon takes the following form:

$$S_{\text{baryon}} = \left(S_{\text{strings}}^{(-2)} + S_{\text{strings}}^{(0)} + S_{\text{strings}}^{(2)} \right) + \left(S_{\text{junction}}^{(-1)} + S_{\text{junction}}^{(1)} \right) + \left(S_{\text{displacement}}^{(1)} + S_{\text{displacement}}^{(2)} \right) + O(\partial^3), \quad (2.16)$$

which we now unpack term by term.

In equation (2.16), the terms $S_{\text{strings}}^{(-2)}$, $S_{\text{strings}}^{(0)}$, and $S_{\text{strings}}^{(2)}$ collect effective actions of the three strings up to order 2. As in the single string case (2.3), the order -2 classical term of three strings is as follows:

$$S_{\text{strings}}^{(-2)} = -l_s^{-2} \int dt \left(\int_0^{L_x} d\sigma + \int_0^{L_y} d\sigma + \int_0^{L_z} d\sigma \right). \quad (2.17)$$

The order 0 term $S_{\text{strings}}^{(0)}$ is the quadratic kinetic action that governs the leading quantum fluctuations on the worldsheets:

$$S_{\text{strings}}^{(0)} = \frac{1}{2} \int dt \int_0^{L_x} d\sigma [(\partial_t x_i)^2 - (\partial_\sigma x_i)^2] + (x \rightarrow y) + (x \rightarrow z). \quad (2.18)$$

At the quark endpoints, the NGBs x_i , y_i , and z_i are subject to the Dirichlet boundary condition (2.5). On the other hand, the rigid geometry of confining strings at the baryon junction leads to the constraints:

$$x_2 + y_2 + z_2 = 0, \quad \text{and} \quad x_j = y_j = z_j \quad \text{for} \quad 3 \leq j \leq d. \quad (2.19)$$

It is convenient to introduce the linear combinations $\xi_i^{[1]} = x_i + y_i + z_i$, $\xi_i^{[2]} = x_i - y_i$, and $\xi_i^{[3]} = x_i + y_i - 2z_i$ for $2 \leq i \leq d$. In these new variables, the geometry constraints (2.19) and the variational principle of (2.18) determine the following boundary condition at $\sigma = 0$:

$$\partial_t \xi_2^{[1]} = \partial_t \xi_j^{[2]} = \partial_t \xi_j^{[3]} = 0, \quad \text{and} \quad \partial_\sigma \xi_2^{[2]} = \partial_\sigma \xi_2^{[3]} = \partial_\sigma \xi_j^{[1]} = 0 \quad \text{for} \quad 3 \leq j \leq d. \quad (2.20)$$

Higher-order corrections to the baryon junction boundary condition (2.20) arise from interaction terms localized at $\sigma = 0$. As we will show in Section 4, these interactions are strongly constrained by Poincaré symmetry and open-closed duality. Finally, the order 2 term $S_{\text{strings}}^{(2)}$ contains the quartic interactions on the worldsheets:

$$S_{\text{strings}}^{(2)} = \frac{l_s^2}{8} \int dt \int_0^{L_x} d\sigma (\partial_t x_i - \partial_\sigma x_i)^2 (\partial_t x_{i'} + \partial_\sigma x_{i'})^2 + (x \rightarrow y) + (x \rightarrow z), \quad (2.21)$$

which follows from the Nambu-Goto action, as in equation (2.3).

The terms $S_{\text{junction}}^{(-1)}$ and $S_{\text{junction}}^{(1)}$ in equation (2.16) describe the worldline dynamics of the baryon junction. Let W_μ denote the spacetime coordinates of the baryon junction point. The leading worldline action compatible with Poincaré symmetry then takes the form:

$$S_{\text{junction}} = -M \int_{\sigma=0} dt \sqrt{-(\partial_t W_\mu)^2} = S_{\text{junction}}^{(-1)} + S_{\text{junction}}^{(1)} + O(\partial^3). \quad (2.22)$$

We have introduced a new EFT parameter M in the action (2.22), which is interpreted as the classical mass of the baryon junction. Expanding the worldline action (2.22) in the NGBs x_i , y_i , and z_i , we find the order -1 term

$$S_{\text{junction}}^{(-1)} = -M \int_{\sigma=0} dt, \quad (2.23)$$

together with the order 1 term

$$S_{\text{junction}}^{(1)} = \frac{Ml_s^2}{18} \int_{\sigma=0} dt [(\partial_t x_j + \partial_t y_j + \partial_t z_j)^2 + (\partial_t x_2 + \partial_t y_2 - 2\partial_t z_2)^2 + 3(\partial_t x_2 - \partial_t y_2)^2] . \quad (2.24)$$

In equation (2.24), we have chosen the linear combinations of x_i , y_i , and z_i that survive the geometry constraint (2.19).

Unlike the open string boundaries reviewed in Section 2.1, the baryon junction is allowed to fluctuate in the longitudinal directions of the confining strings. The longitudinal displacements of the three strings at $\sigma = 0$ are determined by the geometry in figure 1, and are given by

$$\delta X_1 = \frac{l_s}{\sqrt{3}}(z_2 - y_2) , \quad \delta Y_1 = \frac{l_s}{\sqrt{3}}(x_2 - z_2) , \quad \text{and} \quad \delta Z_1 = \frac{l_s}{\sqrt{3}}(y_2 - x_2) . \quad (2.25)$$

These displacements couple to EFT operators that generate infinitesimal deformations of the worldsheet boundary, analogous to the displacement operator in defect conformal field theory [65–67]. For example, let us consider a single confining string whose endpoint fluctuates infinitesimally in the longitudinal direction with $\sigma \geq \delta X_1(t)$. Expanding the worldsheet action (2.3) in powers of δX_1 , we identify the following effective coupling at the boundary:

$$S_{\text{displacement}} = \sum_{n \in \mathbb{N}} \int_{\sigma=0} dt (-\delta X_1)^{n+1} \partial_\sigma^n \left(-\frac{1}{l_s^2} + \frac{1}{2}((\partial_t x_i)^2 - (\partial_\sigma x_i)^2) + O(\partial^4) \right) . \quad (2.26)$$

In the baryon junction case, the longitudinal displacements are promoted to dynamical fields as in equation (2.25), while the worldsheet action up to order 2 is dictated by (2.17), (2.18), and (2.21). The geometric constraint $\delta X_1 + \delta Y_1 + \delta Z_1 = 0$ ensures that the order -1 coupling of the longitudinal fluctuations is trivial. The leading order 1 coupling is therefore

$$S_{\text{displacement}}^{(1)} = \frac{l_s}{2\sqrt{3}} \int_{\sigma=0} dt [(y_2 - z_2)((\partial_t x_i)^2 - (\partial_\sigma x_i)^2) + (z_2 - x_2)((\partial_t y_i)^2 - (\partial_\sigma y_i)^2) + (x_2 - y_2)((\partial_t z_i)^2 - (\partial_\sigma z_i)^2)] , \quad (2.27)$$

followed by the subleading order 2 term,

$$S_{\text{displacement}}^{(2)} = \frac{l_s^2}{12} \int_{\sigma=0} dt [(y_2 - z_2)^2 \partial_\sigma ((\partial_t x_i)^2 - (\partial_\sigma x_i)^2) + (z_2 - x_2)^2 \partial_\sigma ((\partial_t y_i)^2 - (\partial_\sigma y_i)^2) + (x_2 - y_2)^2 \partial_\sigma ((\partial_t z_i)^2 - (\partial_\sigma z_i)^2)] , \quad (2.28)$$

For simplicity, we have combined the longitudinal contributions from the three worldsheets in equations (2.27) and (2.28).

To summarize, we have classified terms in the effective action of the probe baryon up to order 2. We find that the effective action (2.16) is determined by two EFT parameters, namely the classical string tension l_s^{-2} and the classical baryon junction mass M . New EFT parameters may appear at higher orders; for example, the κ_D term in (2.6) at the quark endpoints is of order 3. The quantum fluctuations of the probe baryon are fully controlled by l_s^{-2} and M up to order 2, whose physical implications we will discuss in the upcoming sections.

3 Open-closed duality of baryon junctions

In this section, we establish the open-closed duality for the junctions of confining strings. To set the stage, it is useful to recall the dual channels of a finite open string reviewed in Section 2.2. The open-closed duality identifies the thermal partition function of a probe meson (2.9) with the two-point correlation function of Polyakov loop operators (2.13). We assume that the Polyakov operators (i.e., the quark endpoints of the confining strings) can be decomposed into massive particles in d -dimensional space. By matching the partition function (2.10) with (2.14) via modular transformations, we fix the decomposition coefficients up to their leading orders as in equation (2.15).

We now turn to the probe baryon case in figure 1. In the open channel, the baryon partition function \mathcal{Z} takes the form

$$\text{open channel : } \mathcal{Z} = \sum_{E_{\text{baryon}}} e^{-\beta E_{\text{baryon}}} , \quad (3.1)$$

where E_{baryon} denotes the energy eigenvalues of the baryon states. As in Section 2.2, the partition function can be computed from the effective action (2.16) by Wick rotating $t \rightarrow -i\tau$ and compactifying $\tau \sim \tau + \beta$. We carry out this calculation in Sections 3.1 and 4.

With three external quarks, we argue that the closed channel of the baryon partition function is given by the three-point function of Polyakov operators:

$$\text{closed channel : } \mathcal{Z} = \langle \Omega(\vec{X})\Omega(\vec{Y})\Omega(\vec{Z}) \rangle . \quad (3.2)$$

In equation (3.2), \vec{X} , \vec{Y} , and \vec{Z} denote positions in d -dimensional space. We adopt the convention

$$\vec{X} = (L_x, 0, \dots) , \quad \vec{Y} = \left(-\frac{1}{2}L_y, \frac{\sqrt{3}}{2}L_y, \dots\right) , \quad \text{and} \quad \vec{Z} = \left(-\frac{1}{2}L_z, -\frac{\sqrt{3}}{2}L_z, \dots\right) , \quad (3.3)$$

where we have omitted the $(d-2)$ perpendicular directions, and the Fermat–Weber point of the $\vec{X}\vec{Y}\vec{Z}$ triangle is at the origin. The three-point function (3.2) defines a nontrivial observable when \mathbb{Z}_3 is a 1-form symmetry subgroup of the underlying gauge theory. Our discussion applies, for instance, to $SU(3N)$ and $PSU(3N)$ pure Yang-Mills theories in $(3+1)$ dimensions⁴.

In Sections 3.2 and 4, we show that the three-point function (3.2) is dominated by the tree-level s -wave scattering of the massive particles Φ_a described in (2.12). By matching the dual channels (3.1) and (3.2) via modular transformations, we determine the interaction vertices in the potential function $V(\Phi_a, \Phi_b, \dots)$ that governs the s -wave scattering. In the rest of this section, we elaborate on this calculation up to order 1, where 1-loop corrections on the worldsheets are concerned. With simplifications, we continue this calculation to order 2 in Section 4.

⁴The $PSU(3N)$ Yang-Mills theories in $(3+1)$ dimensions have a magnetic 1-form symmetry $\mathbb{Z}_{3N} \supseteq \mathbb{Z}_3$. In these theories, confining strings end on magnetic monopoles corresponding to 't Hooft line operators.

3.1 Partition function of the probe baryon

We begin by considering the Euclidean path-integral of the effective action (2.16)

$$\mathcal{Z} = \int \mathcal{D}x_i \mathcal{D}y_i \mathcal{D}z_i e^{-S_{\text{baryon}}} , \quad (3.4)$$

with Euclidean time compactified on a circle of circumference $\beta = 2\pi R$. This path-integral admits the following perturbative expansion:

$$\begin{aligned} \mathcal{Z} = e^{-S_{\text{strings}}^{(-2)} - S_{\text{junction}}^{(-1)}} \mathcal{Z}^{(0)} & \left[1 - \langle S_{\text{junction}}^{(1)} \rangle - \langle S_{\text{strings}}^{(2)} \rangle - \langle S_{\text{displacement}}^{(2)} \rangle \right. \\ & \left. + \frac{1}{2} \langle (S_{\text{junction}}^{(1)})^2 \rangle + \frac{1}{2} \langle (S_{\text{displacement}}^{(1)})^2 \rangle + O(\partial^3) \right] , \end{aligned} \quad (3.5)$$

where we have defined

$$\mathcal{Z}^{(0)} \equiv \int \mathcal{D}x_i \mathcal{D}y_i \mathcal{D}z_i e^{-S_{\text{strings}}^{(0)}} , \quad \text{and} \quad \langle \dots \rangle \equiv \frac{1}{\mathcal{Z}^{(0)}} \int \mathcal{D}x_i \mathcal{D}y_i \mathcal{D}z_i (\dots) e^{-S_{\text{strings}}^{(0)}} . \quad (3.6)$$

The classical contributions to the path-integral are given by $S_{\text{strings}}^{(-2)}$ in equation (2.17) and $S_{\text{junction}}^{(-1)}$ in equation (2.23). We readily find that

$$S_{\text{strings}}^{(-2)} = \frac{2\pi R}{l_s^2} (L_x + L_y + L_z) , \quad \text{and} \quad S_{\text{junction}}^{(-1)} = 2\pi R M . \quad (3.7)$$

We have organized the quantum fluctuations in the path-integral (3.5) according to their EFT order, where $\mathcal{Z}^{(0)}$ is the leading order 0 contribution. Among the higher-order corrections, we note that the expectation values of parity-odd terms vanish. For example, $\langle S_{\text{displacement}}^{(1)} \rangle = 0$ and $\langle S_{\text{junction}}^{(1)} S_{\text{displacement}}^{(1)} \rangle = 0$. In the rest of this section, we compute $\mathcal{Z}^{(0)}$ and $\langle S_{\text{junction}}^{(1)} \rangle$, thereby fixing the partition function up to order 1. We will elaborate on the order 2 corrections $\langle S_{\text{strings}}^{(2)} \rangle$, $\langle S_{\text{displacement}}^{(2)} \rangle$, $\langle (S_{\text{junction}}^{(1)})^2 \rangle$, and $\langle (S_{\text{displacement}}^{(1)})^2 \rangle$ in Section 4.

The order 0 effective action (2.18) is simply the free kinetic action for the NGBs x_i , y_i , and z_i . The partition function $\mathcal{Z}^{(0)}$ with the baryon junction condition (2.19) and (2.20) can be evaluated as follows [28, 30, 31]: we first fix the spacetime trajectory of the point-like junction, then integrate over the NGB fluctuations around the saddle point determined by this trajectory, and finally perform the quantum-mechanical path-integral over the junction worldline. In the static gauge, the baryon junction worldline in $(d+1)$ -dimensional spacetime $W_\mu = (W_0, \vec{W})$ is parameterized as

$$W_0 = \tau , \quad \vec{W} = l_s \vec{w}(\tau) = l_s (w_1(\tau), w_2(\tau), \dots, w_d(\tau)) . \quad (3.8)$$

The trajectory $\vec{w}(\tau)$ sets the boundary profiles for the NGBs x_i , y_i , and z_i , as illustrated by the geometry in figure 1. We take the following convention that at the junction $\sigma = 0$:

$$\begin{aligned} x_2 = w_2 , \quad y_2 = -\frac{\sqrt{3}}{2} w_1 - \frac{1}{2} w_2 , \quad z_2 = \frac{\sqrt{3}}{2} w_1 - \frac{1}{2} w_2 , \\ \text{and} \quad x_j = y_j = z_j = w_j \quad \text{for} \quad 3 \leq j \leq d . \end{aligned} \quad (3.9)$$

The saddle point of the NGB fields subject to the boundary condition (3.9) and action (2.18) is solved by the free theory equation of motion. For convenience, we introduce the Dirichlet-Dirichlet Green's function on a cylinder $G(\sigma, \sigma', \tau; q)$ as in equation (C.2), and define the modular parameters q_x , q_y , and q_z as

$$q_x \equiv e^{-\frac{2\pi^2 R}{L_x}}, \quad q_y \equiv e^{-\frac{2\pi^2 R}{L_y}}, \quad \text{and} \quad q_z \equiv e^{-\frac{2\pi^2 R}{L_z}}. \quad (3.10)$$

The saddle point configurations of the NGBs x_i^* , y_i^* , and z_i^* then take the form

$$\begin{aligned} (x_2^*, x_j^*) &= \int_{\sigma'=0} d\tau' \partial_{\sigma'} G(\sigma, \sigma', \tau - \tau'; q_x) (w_2(\tau'), w_j(\tau')), \\ (y_2^*, y_j^*) &= \int_{\sigma'=0} d\tau' \partial_{\sigma'} G(\sigma, \sigma', \tau - \tau'; q_y) \left(-\frac{\sqrt{3}}{2} w_1(\tau') - \frac{1}{2} w_2(\tau'), w_j(\tau') \right), \\ (z_2^*, z_j^*) &= \int_{\sigma'=0} d\tau' \partial_{\sigma'} G(\sigma, \sigma', \tau - \tau'; q_z) \left(\frac{\sqrt{3}}{2} w_1(\tau') - \frac{1}{2} w_2(\tau'), w_j(\tau') \right). \end{aligned} \quad (3.11)$$

For free theories, the fluctuation spectrum is independent of the Gaussian saddle point around which one expands [68, 69]. The path-integral therefore factorizes into two pieces: the partition function of three confining strings with Dirichlet boundary conditions on both ends, and the path-integral over the baryon junction worldline, governed by the saddle point action. Specifically, we find that

$$\mathcal{Z}^{(0)} = \frac{1}{(\eta(q_x)\eta(q_y)\eta(q_z))^{d-1}} \int \mathcal{D}\vec{w} \exp\left(-S_{\text{strings}}^{(0)}(x_i^*, y_i^*, z_i^*)\right). \quad (3.12)$$

In equation (3.12), $S_{\text{strings}}^{(0)}(x_i^*, y_i^*, z_i^*)$ denotes the order 0 effective action (2.18) evaluated at the saddle point (3.11). As a functional of the junction trajectory $\vec{w}(\tau)$, it gives the trapping potential arising from the backreaction of confining strings. See equations (C.4) and (C.5) in Appendix C, for the explicit form of $S_{\text{strings}}^{(0)}(x_i^*, y_i^*, z_i^*)$. We carry out the Gaussian path-integral in equation (3.12) and find that

$$\begin{aligned} \mathcal{Z}^{(0)} &= \frac{(L_x^{-1} + L_y^{-1} + L_z^{-1})^{1-\frac{d}{2}}}{(2\pi R)^{\frac{d}{2}} (\eta(q_x)\eta(q_y)\eta(q_z))^{d-1}} \sqrt{\frac{L_x L_y L_z}{L_x + L_y + L_z}} \prod_{n \in \mathbb{N}^+} \left[\tanh\left(\frac{nL_x}{R}\right) \right. \\ &\quad \left. \times \tanh\left(\frac{nL_y}{R}\right) \tanh\left(\frac{nL_z}{R}\right) \frac{\left(\coth\left(\frac{nL_x}{R}\right) + \coth\left(\frac{nL_y}{R}\right) + \coth\left(\frac{nL_z}{R}\right)\right)^{2-d}}{\tanh\left(\frac{nL_x}{R}\right) + \tanh\left(\frac{nL_y}{R}\right) + \tanh\left(\frac{nL_z}{R}\right)} \right]. \end{aligned} \quad (3.13)$$

The same method extends to the order 1 correction $\langle S_{\text{junction}}^{(1)} \rangle$, which is given by the quantum mechanical path-integral:

$$\langle S_{\text{junction}}^{(1)} \rangle = \frac{Ml_s^2}{2} \frac{\int \mathcal{D}\vec{w} (\partial_\tau \vec{w})^2 \exp\left(-S_{\text{strings}}^{(0)}(x_i^*, y_i^*, z_i^*)\right)}{\int \mathcal{D}\vec{w} \exp\left(-S_{\text{strings}}^{(0)}(x_i^*, y_i^*, z_i^*)\right)}. \quad (3.14)$$

We thereby find the following infinite sum representation for $\langle S_{\text{junction}}^{(1)} \rangle$

$$\begin{aligned} \langle S_{\text{junction}}^{(1)} \rangle = \frac{Ml_s^2}{R} \sum_{n \in \mathbb{N}^+} & \left[\frac{(d-2)n}{\coth\left(\frac{nL_x}{R}\right) + \coth\left(\frac{nL_y}{R}\right) + \coth\left(\frac{nL_z}{R}\right)} + \frac{4n}{3} \tanh\left(\frac{nL_x}{R}\right) \right. \\ & \left. \times \tanh\left(\frac{nL_y}{R}\right) \tanh\left(\frac{nL_z}{R}\right) \frac{\coth\left(\frac{nL_x}{R}\right) + \coth\left(\frac{nL_y}{R}\right) + \coth\left(\frac{nL_z}{R}\right)}{\tanh\left(\frac{nL_x}{R}\right) + \tanh\left(\frac{nL_y}{R}\right) + \tanh\left(\frac{nL_z}{R}\right)} \right]. \end{aligned} \quad (3.15)$$

To the best of our knowledge, the partition function contributions (3.13) and (3.15) with generic L_x , L_y , and L_z do not admit a closed form. See Appendix B for further discussion of cases in which the ratios of confining string lengths are rational. We note a particularly simple case:

$$\text{equilateral baryon : } L_x = L_y = L_z = L, \quad \text{with } q \equiv e^{-\frac{2\pi^2 R}{L}}. \quad (3.16)$$

For equilateral baryons, the contributions (3.13) and (3.15) can be written in terms of (quasi-)modular forms of the parameters q and \sqrt{q} as follows:

$$\begin{aligned} \text{equilateral baryon : } \mathcal{Z}^{(0)} &= \frac{1}{(\eta(\sqrt{q}))^d (\eta(q))^{d-3}}, \quad \text{and} \\ \langle S_{\text{junction}}^{(1)} \rangle &= \frac{(d+2)Ml_s^2}{144L} \ln q (2E_2(q) - E_2(\sqrt{q})), \end{aligned} \quad (3.17)$$

in agreement with [1].

3.2 *S*-wave scattering

Having analyzed the open channel in the last section, we now turn to the closed channel representation (3.2) of the baryon partition function. See also the discussion in [1].

Higher-point functions of the Polyakov loop operators are governed by the potential $V(\Phi_a, \Phi_b, \dots)$ in the effective action (2.12). For trivalent baryon junctions in figure 1, we have assumed that the underlying $(d+1)$ -dimensional gauge theory is endowed with a \mathbb{Z}_3 1-form symmetry, either exact in the UV or emergent in the IR. Upon dimensional reduction, this 1-form symmetry descends to a \mathbb{Z}_3 0-form acting on the complex scalar fields Φ_a in d -dimensional space. We note that the \mathbb{Z}_3 -symmetric potential $V(\Phi_a, \Phi_b, \dots)$ admits cubic interaction vertices of the form:

$$\begin{aligned} V(\Phi_a, \Phi_b, \dots) \supset \frac{1}{2} \left(\frac{3}{2\pi} \right)^{\frac{d}{2}} (\sqrt{\pi} l_s)^{\frac{d-3}{2}} \sum_{a,b,c} \sqrt{E_a^{\text{closed}} E_b^{\text{closed}} E_c^{\text{closed}}} \\ \times \left[C_{abc}^{(0)} \Phi_a \Phi_b \Phi_c + C_{abc}^{(2)} \partial_\nu \Phi_a \partial_\nu \Phi_b \Phi_c + (\text{c.c.}) + O(\partial^4) \right], \end{aligned} \quad (3.18)$$

where $C_{abc}^{(n)}$ denote the order n cubic coupling constants, fully symmetric in the massive mode indices a, b, c . The various prefactors in equation (3.18) are chosen so that $C_{abc}^{(0)}$ are dimensionless and geometric factors are canceled, as we will see below.

At tree-level in the perturbation theory, these interaction vertices determine scattering amplitudes between massive particles in d -dimensional space. See also figure 2. In particular, the coupling constants $C_{abc}^{(0)}$ are associated with the *s*-wave scattering. Likewise,

$C_{abc}^{(2)}$ correspond to the p -wave scattering, while higher-spin scatterings (e.g. d -wave) arise at order $O(\partial^4)$ in the potential (3.18). We find that the following interaction vertices become total derivatives upon using the equations of motion:

$$2 \sum_{a,b,c} C_{abc}^{(2)} \partial_\nu \Phi_a \partial_\nu \Phi_b \Phi_c = \sum_{a,b,c} C_{abc}^{(2)} \left(\partial_\nu (\partial_\nu \Phi_a \Phi_b \Phi_c) - (\partial_\nu^2 \Phi_a) \Phi_b \Phi_c \right). \quad (3.19)$$

As far as local kinetic terms are concerned, the coupling constants $C_{abc}^{(2)}$ can be removed by redefining $C_{abc}^{(0)}$ and the higher-spin terms. We therefore find that the tree-level amplitudes in the three-point function $\langle \Phi_a \Phi_b \Phi_c \rangle$ are determined entirely by s -wave scatterings up to order 3.

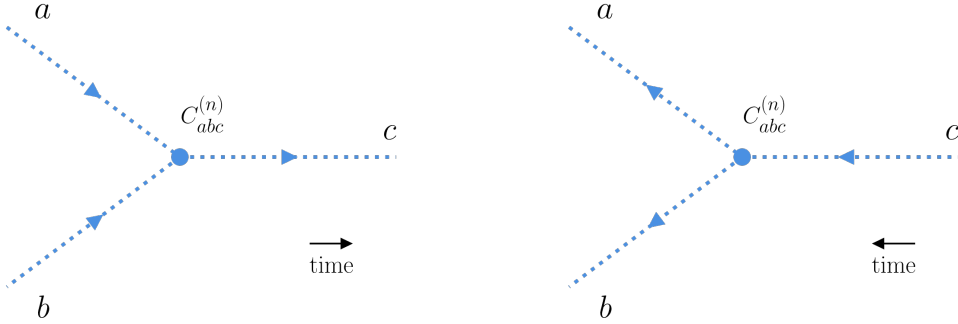


Figure 2: Tree-level scattering amplitudes of massive modes in the closed channel. Interpreting one direction of the d -dimensional space as time, the cubic interaction vertices in equation (3.18) describe the $2 \rightarrow 1$ fusion process (Left) and the $1 \rightarrow 2$ decay process (Right). The external legs in this figure are generally off-shell, since all modes in the closed channel have approximately the same mass (2.4).

As in Section 2.2, we argue that the loop contributions in the three-point function (3.2) are exponentially suppressed. The partition function up to the order 3 is thereby given by the Feynman integral

$$\begin{aligned} \mathcal{Z} = \sum_{a,b,c} \int d^d \vec{W} l_s^{-d} C_{abc}^{(0)} v_a v_b v_c & \left(\frac{(E_a^{\text{closed}})^{\frac{d}{2}} l_s^{d-1}}{\sqrt{\pi} (2L_{wx})^{\frac{d-2}{2}}} K_{\frac{d-2}{2}}(E_a^{\text{closed}} L_{wx}) \right) \\ & \times \left(\frac{(E_b^{\text{closed}})^{\frac{d}{2}} l_s^{d-1}}{\sqrt{\pi} (2L_{wy})^{\frac{d-2}{2}}} K_{\frac{d-2}{2}}(E_b^{\text{closed}} L_{wy}) \right) \left(\frac{(E_c^{\text{closed}})^{\frac{d}{2}} l_s^{d-1}}{\sqrt{\pi} (2L_{wz})^{\frac{d-2}{2}}} K_{\frac{d-2}{2}}(E_c^{\text{closed}} L_{wz}) \right), \end{aligned} \quad (3.20)$$

where $L_{wx} = |\vec{X} - \vec{W}|$, $L_{wy} = |\vec{Y} - \vec{W}|$, and $L_{wz} = |\vec{Z} - \vec{W}|$. In equation (3.20), we have employed the decomposition (2.11) of the Polyakov operators and used the massive propagator (2.13) derived from the effective action (2.12). The Feynman integral is heavily dominated by its saddle point contribution, which we examine in detail in Section 4. For later convenience, we introduce the dual modular parameters:

$$\tilde{q}_x \equiv e^{-\frac{2L_x}{R}}, \quad \tilde{q}_y \equiv e^{-\frac{2L_y}{R}}, \quad \text{and} \quad \tilde{q}_z \equiv e^{-\frac{2L_z}{R}}. \quad (3.21)$$

The partition function then takes the form [1]

$$\begin{aligned} \mathcal{Z} = & \left(\frac{3\pi R}{L_x + L_y + L_z} \right)^{d-\frac{3}{2}} \left(\frac{(L_x + L_y + L_z)^2}{3(L_x L_y + L_y L_z + L_z L_x)} \right)^{\frac{d}{2}-1} \\ & \times \frac{e^{-2\pi R(L_x + L_y + L_z)/l_s^2}}{2^{\frac{d}{2}} (\tilde{q}_x \tilde{q}_y \tilde{q}_z)^{\frac{d-1}{24}}} \sum_{a,b,c} \left(C_{abc}^{(0)} + O(\partial^2) \right) v_a v_b v_c \tilde{q}_x^{n_a} \tilde{q}_y^{n_b} \tilde{q}_z^{n_c}, \end{aligned} \quad (3.22)$$

where n_a, n_b, n_c are the integer excitation levels given in equation (2.4).

The open-closed duality of the baryon junctions identifies the two representations (3.5) and (3.22) of the partition function. This allows us to fix the coupling constants $C_{abc}^{(0)}$ by consistency conditions, even though the underlying confining gauge theory is strongly coupled. Indeed, the open channel terms in equations (3.13) and (3.15) admit expansions in $\tilde{q}_x, \tilde{q}_y,$ and \tilde{q}_z using the modular transformation. Putting together $\mathcal{Z}^{(0)}, \langle S_{\text{junction}}^{(1)} \rangle,$ and the classical contribution (3.7) to the partition function, we find the four coupling constants involving the closed string states $\mathbf{0}$ and $\mathbf{1}$:

$$\begin{aligned} C_{\mathbf{000}}^{(0)} &= e^{-2\pi RM} \left[1 + \frac{(d+2)Ml_s^2}{36R} + O(R^{-2}) \right], \\ C_{\mathbf{001}}^{(0)} &= \frac{e^{-2\pi RM}}{3\sqrt{d-1}} \left[(d-3) + \frac{(d+2)(d+21)Ml_s^2}{36R} + O(R^{-2}) \right], \\ C_{\mathbf{011}}^{(0)} &= \frac{e^{-2\pi RM}}{9(d-1)} \left[(d^2 - 2d + 5) + \frac{(d^3 + 48d^2 - 143d - 278)Ml_s^2}{36R} + O(R^{-2}) \right], \\ C_{\mathbf{111}}^{(0)} &= \frac{e^{-2\pi RM}}{27(d-1)^{\frac{3}{2}}} \left[(d-3)(d^2 + 6d - 19) \right. \\ & \quad \left. + \frac{(d^4 + 77d^3 - 319d^2 + 1495d - 1470)Ml_s^2}{36R} + O(R^{-2}) \right]. \end{aligned} \quad (3.23)$$

We note that the coupling constants in (3.23) depend on the intrinsic EFT parameters l_s and M , as well as on the radius R of Polyakov loops. They are independent of the operator positions (i.e., $L_x, L_y,$ and L_z), as expected from the locality of the interaction vertices in (3.18). We will return to this point in Section 4, where higher-order corrections are included.

3.3 An accidental \mathbb{Z}_2 symmetry

We have shown that the interaction vertices in the effective action of propagating closed strings can be determined using open-closed duality. In particular, s -wave scatterings of these closed strings are associated with the scale $\Lambda_{s\text{-wave}}$ that generally obeys

$$(\Lambda_{s\text{-wave}})^{3-\frac{d}{2}} \sim l_s^{\frac{d-3}{2}} \sqrt{E_a^{\text{closed}} E_b^{\text{closed}} E_c^{\text{closed}} C_{abc}^{(0)}} \sim R^{\frac{3}{2}} l_s^{\frac{d-9}{2}} e^{-2\pi RM}. \quad (3.24)$$

Notably, the baryon junction mass M sets a non-perturbative factor $e^{-2\pi RM}$ that governs the interactions between long strings. The perturbative description applies to the effective action (2.12) given that $M \geq 0$. Nevertheless, consistency by itself places no strict bounds on the junction mass M . See [1] for a relevant discussion.

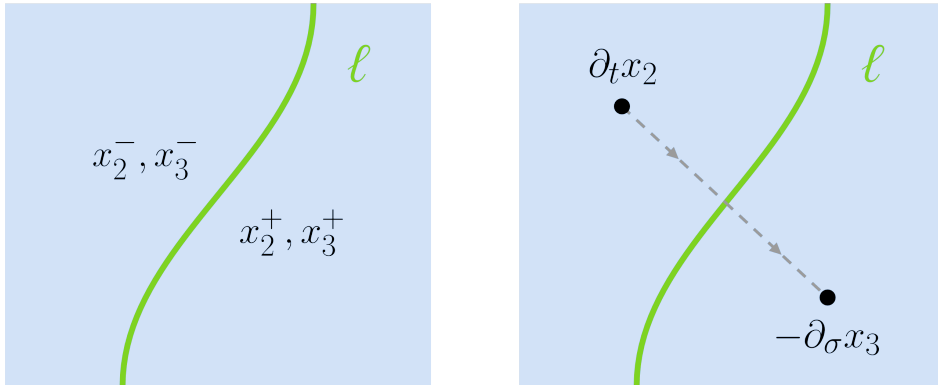


Figure 3: Topological defect line \mathcal{D} on the confining string worldsheet. Left: the NGB field profiles are taken to be discontinuous across the line ℓ , and the defect action is given by the bilinear coupling between x_i^- and x_i^+ . Right: local operators transform according to equation (3.26) upon crossing the defect line. The \mathbb{Z}_2 symmetry transformation rule can be schematically written as $(\partial_t x_2, \partial_\sigma x_2) \xrightarrow{\mathcal{D}} (-\partial_\sigma x_3, -\partial_t x_3) \xrightarrow{\mathcal{D}} (\partial_t x_2, \partial_\sigma x_2)$.

Interestingly, the effective string theory in $(3+1)$ -dimensional spacetime (i.e., $d=3$) presents an accidental symmetry that is broken by the junction mass M . To see this, we consider a class of line defects living on the confining string worldsheet with the effective action (2.3). The defect \mathcal{D} is defined by coupling the NGB fields across the line manifold ℓ as follows:

$$\mathcal{D}(\ell) \equiv \exp \left(i \int_{\ell} (x_2^- dx_3^+ - x_3^- dx_2^+) \right) = \exp \left(i S_{\text{defect}}^{(0)} \right), \quad (3.25)$$

where x_i^- denotes the field profile on the left-hand side of ℓ , while x_i^+ denotes the profile on the right-hand side. See also figure 3. This construction is analogous to the T-duality defects in the 2-dimensional free compact boson theory [70–73]. The insertion of the defect \mathcal{D} preserves the transverse rotation group $SO(2)$ and modifies the equations of motion for the NGB fields. It follows from the variational principle that the fields on the two sides of the defect are matched according to

$$(\partial_t x_2^-, \partial_\sigma x_2^-, \partial_t x_3^-, \partial_\sigma x_3^-) = (\partial_\sigma x_3^+, \partial_t x_3^+, -\partial_\sigma x_2^+, -\partial_t x_2^+) . \quad (3.26)$$

For the probe baryon configurations shown in figure 1, we can similarly define defects \mathcal{D} on the confining string worldsheets using variables y_i^\pm and z_i^\pm , respectively.

The free theory limit of the baryon effective action (2.16) is governed by the quadratic kinetic term (2.18) and the junction condition (2.20). One readily verifies that the worldsheet stress-energy tensor is continuous across \mathcal{D} in this limit. Equation (3.25) therefore defines a topological defect line in the free theory, which generates a \mathbb{Z}_2 global symmetry on the worldsheet. In particular, the symmetry transformation rule for local operators is given by (3.26).⁵

⁵Local vertex operators (e.g., $\exp(ik_i x_i)$) are mapped to semi-local twist operators under this \mathbb{Z}_2 sym-

Notably, the baryon junction condition (2.20) preserves the \mathbb{Z}_2 symmetry generated by the topological defect line \mathcal{D} .⁶ The key observation is as follows: the linear combinations of NGB fields $\xi_2^{[1]}$, $\xi_3^{[2]}$, and $\xi_3^{[3]}$ satisfy Dirichlet boundary conditions at the junction, while the other combinations $\xi_2^{[2]}$, $\xi_2^{[3]}$, and $\xi_3^{[1]}$ satisfy Neumann boundary conditions. The \mathbb{Z}_2 symmetry (3.25) exchanges Dirichlet and Neumann conditions and acts by a $\pi/2$ rotation on the spatial indices transverse to the confining string, therefore leaving the junction condition invariant. In the free theory limit, the baryon junction worldline can be merged with the defect \mathcal{D} across the three connected worldsheets as in figure 4. The \mathbb{Z}_2 symmetry acts on operators localized at the baryon junction through the topological intersection of the junction worldline with the line defects.

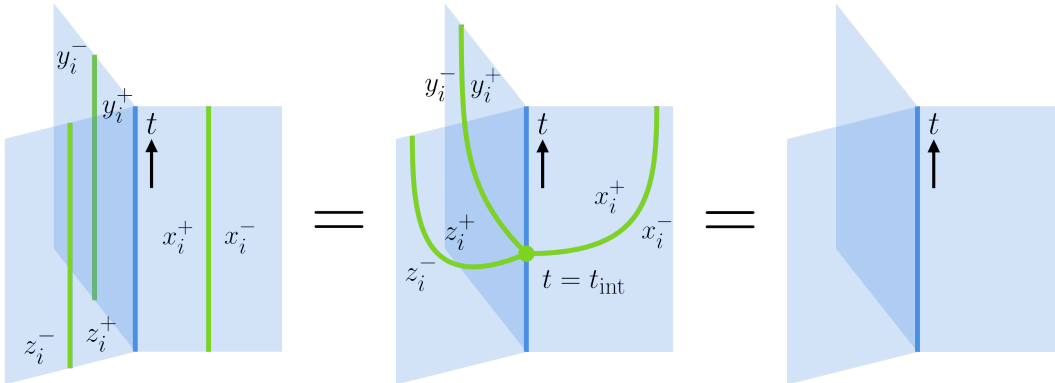


Figure 4: Merging the topological defect lines with the baryon junction worldline.

We now examine whether the \mathbb{Z}_2 symmetry generated by the defect \mathcal{D} persists in the full effective theory (2.16). On the confining string worldsheets, we note that the quartic interaction in equation (2.21) is invariant under the \mathbb{Z}_2 transformation (3.26). The leading symmetry breaking interaction on the worldsheets arises at order 4 and is controlled by the Polyakov–Kleinert rigidity term.

On the other hand, the baryon junction worldline preserves the \mathbb{Z}_2 symmetry if its intersection with defect \mathcal{D} remains topological. We first note that coupling the worldsheets on the two sides of the defect using (3.25) requires the longitudinal displacements δX_1 , δY_1 , and δZ_1 in (2.25) to be continuous across the defect line. This leads to the following consistency condition at the intersection point $t = t_{\text{int}}$ (see figure 4):

$$\text{gluing condition} : x_2^+ = x_2^-, y_2^+ = y_2^-, \text{ and } z_2^+ = z_2^- \text{ at } (t, \sigma) = (t_{\text{int}}, 0), \quad (3.27)$$

metry. These twist operators are characterized by the field monodromy $x_i \rightarrow x_i + \text{const}$ around the operator insertion.

⁶For effective string theories in $(d+1)$ -dimensional spacetime, we can analogously define a line defect that preserves the transverse rotation group $SO(d-1)$ as follows:

$$\mathcal{D}'(\ell) \equiv \exp\left(i \int_{\ell} x_i^- dx_i^+\right), \text{ where } 2 \leq i \leq d.$$

The baryon junction condition (2.20), however, is not invariant under the symmetry generated by \mathcal{D}' .

which can be implemented using Lagrange multipliers at the intersection point.

We consider the worldline stress-energy tensor \tilde{T} [74], defined by the local divergence of the worldsheet stress-energy tensors $T_{\alpha\beta}[x_i]$, $T_{\alpha\beta}[y_i]$, and $T_{\alpha\beta}[z_i]$ as follows:

$$\partial^\alpha T_{\alpha t}[x_i] + \partial^\alpha T_{\alpha t}[y_i] + \partial^\alpha T_{\alpha t}[z_i] = -\delta(\sigma)\partial_t\tilde{T} . \quad (3.28)$$

The operator \tilde{T} represents the energy stored at the baryon junction, which vanishes in the free theory limit. In the full effective theory, \tilde{T} receives corrections from the actions (2.24), (2.27), (2.28), and other higher-order terms. For example, the contribution from longitudinal displacements on the X -string follows from (2.26) and takes the form

$$\tilde{T} \supset \sum_{n \in \mathbb{N}} (-\delta X_1)^{n+1} \partial_\sigma^n \left(\frac{1}{l_s^2} + \frac{1}{2} ((\partial_t x_i)^2 + (\partial_\sigma x_i)^2) + O(\partial^4) \right) . \quad (3.29)$$

Using the transformation rule (3.26) and the condition (3.27), we find that the corrections to the stress-energy tensor \tilde{T} in (3.29) are continuous across the intersection point $t = t_{\text{int}}$ up to order 2. The discontinuity at $t = t_{\text{int}}$ arises from the worldline kinetic term (2.24) and is given by

$$\begin{aligned} \tilde{T}^+ - \tilde{T}^- = \frac{M l_s^2}{18} & \left[(\partial_t x_3^+ + \partial_t y_3^+ + \partial_t z_3^+)^2 - (\partial_\sigma x_2^+ + \partial_\sigma y_2^+ + \partial_\sigma z_2^+)^2 \right. \\ & + (\partial_t x_2^+ + \partial_t y_2^+ - 2\partial_t z_2^+)^2 - (\partial_\sigma x_3^+ + \partial_\sigma y_3^+ - 2\partial_\sigma z_3^+)^2 \\ & \left. + 3(\partial_t x_2^+ - \partial_t y_2^+)^2 - 3(\partial_\sigma x_3^+ - \partial_\sigma y_3^+)^2 \right] + O(\partial^4) , \end{aligned} \quad (3.30)$$

where \tilde{T}^+ and \tilde{T}^- denote the stress-energy tensor evaluated on the two sides of the intersection point. The discontinuity (3.30) quantifies the obstruction to moving the intersection point topologically along the baryon junction worldline, thereby signaling the \mathbb{Z}_2 symmetry breaking.

We conclude that the baryon junction mass M is the leading parameter that breaks the \mathbb{Z}_2 symmetry (3.25) in the $(3+1)$ -dimensional effective string theory. Unlike the boundary parameters in (2.6) and (2.8), the baryon junction mass can be defined without reference to external probes (e.g., static quarks) and is therefore intrinsic to the underlying UV theory. If the \mathbb{Z}_2 symmetry is exactly realized in the UV theory, it imposes strong constraints on the baryon junction mass, forcing $M = 0$.

In the closed channel, the \mathbb{Z}_2 symmetry (3.25) constrains the interaction vertices in the effective potential $V(\Phi_a, \Phi_b, \dots)$ and implies selection rules for scattering processes. For example, the closed string ground state $\mathbf{0}$ is even under the \mathbb{Z}_2 transformation, while the excited state $\mathbf{1}$ is odd. By the \mathbb{Z}_2 symmetry, the coupling constants in (3.18) must satisfy

$$C_{\mathbf{001}}^{(0)} = C_{\mathbf{111}}^{(0)} = 0 , \quad (3.31)$$

in agreement with the explicit results (3.23) with $d = 3$ and $M = 0$. We will examine these symmetry constraints further in Section 4, where nonlinear corrections are taken into account. Finally, we note that the s -wave scatterings of closed strings in $(3+1)$ -dimensional spacetime are associated with different scales. For a generic baryon junction M , the \mathbb{Z}_2 symmetry preserving (SP) and symmetry breaking (SB) scales are respectively

$$\Lambda_{s\text{-wave}}^{\text{SP}} \sim R l_s^{-2} e^{-\frac{4\pi}{3} R M} , \quad \text{and} \quad \Lambda_{s\text{-wave}}^{\text{SB}} \sim M^{\frac{2}{3}} R^{\frac{1}{3}} l_s^{-\frac{2}{3}} e^{-\frac{4\pi}{3} R M} . \quad (3.32)$$

4 Nonlinear corrections

In this section, we extend the open-closed duality analysis of the baryon junction to the next order in the effective string theory. To keep the discussion streamlined, we have moved the technical details of the calculations in this section to Appendix C.

In the open channel (3.1), the order 2 contributions to the probe baryon partition function include $\langle S_{\text{displacement}}^{(2)} \rangle$, $\langle S_{\text{strings}}^{(2)} \rangle$, $\langle (S_{\text{junction}}^{(1)})^2 \rangle$, and $\langle (S_{\text{displacement}}^{(1)})^2 \rangle$. These terms represent nonlinear corrections to the NGB fields x_i , y_i , and z_i , which can be computed using worldsheet loop diagrams (see figure 5). We present these results in Section 4.1.

In the closed channel (3.2), the partition function remains dominated by s -wave scattering and is given by the tree-level Feynman integral (3.20) up to order 2. By evaluating the integral (3.20) perturbatively around its saddle point, we identify the $O(R^{-2})$ corrections to the coupling constants (3.23). We elaborate on this computation in Section 4.2.

Throughout this section, we will focus on the equilateral baryon configuration (3.16). This allows us to express the results in terms of (quasi-)modular forms of $q = \exp(-2\pi^2 R/L)$ and $\tilde{q} = \exp(-2L/R)$. Nevertheless, our analysis generalizes straightforwardly to other probe baryon configurations.

4.1 Regularized corrections to the partition function

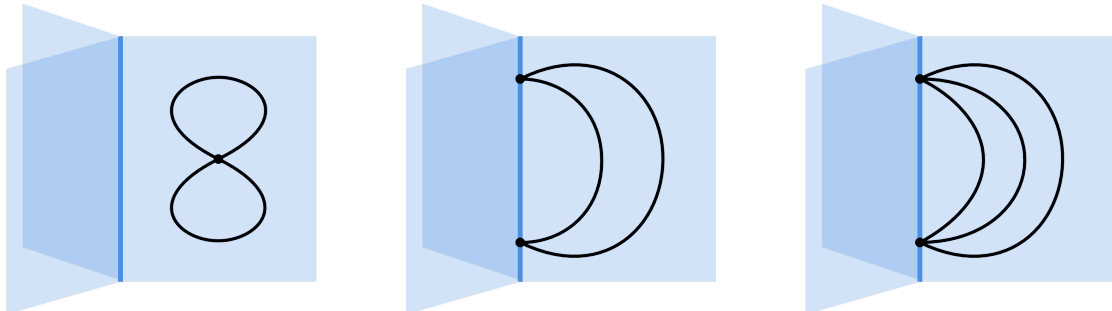


Figure 5: Worldsheet loop diagrams. The black lines denote the propagators of the NGB fields x_i , y_i , and z_i . See equations (C.2), (C.3), (C.6), and (C.7) in Appendix C for the explicit forms of these propagators. Left: $\langle S_{\text{strings}}^{(2)} \rangle$ is given by the 2-loop diagrams on the confining string worldsheets; Middle: $\langle (S_{\text{junction}}^{(1)})^2 \rangle$ is given by the 1-loop diagrams on the baryon junction worldline; Right: $\langle (S_{\text{displacement}}^{(1)})^2 \rangle$ is given by the 2-loop diagrams on the baryon junction worldline.

As shown in figure 5, the order 2 nonlinear corrections to the partition function (3.5) are evaluated by loop diagrams either on confining string worldsheets or localized on the baryon junction worldline. These diagrams correspond to the coincident-point limits of various Green's functions and their integrals, which we review in Appendix C. In general, the loop integrals in $\langle S_{\text{displacement}}^{(2)} \rangle$, $\langle S_{\text{strings}}^{(2)} \rangle$, $\langle (S_{\text{junction}}^{(1)})^2 \rangle$, and $\langle (S_{\text{displacement}}^{(1)})^2 \rangle$ are UV

divergent. We adopt the zeta-function regularization and extract the finite contribution from these loop integrals.

We start with the quartic interaction (2.28) at the baryon junction arising from longitudinal displacements. For the equilateral baryon configuration (3.16), we find by explicit calculation that

$$\langle S_{\text{displacement}}^{(2)} \rangle = 0 . \quad (4.1)$$

See also equations (C.8) and (C.9). With zeta-function regularization, equation (4.1) also holds for general configurations of the probe baryon as in figure 1.

The quartic interaction (2.21) on the confining string worldsheets follows from the Nambu–Goto action. Using zeta-function regularization, we obtain $\langle S_{\text{strings}}^{(2)} \rangle$ in terms of the Eisenstein series (A.2) as follows

$$\begin{aligned} \langle S_{\text{strings}}^{(2)} \rangle &= \frac{\pi l_s^2}{13824L^2} (\ln q) \left[2(d+2)E_4(\sqrt{q}) + 4(d-3)(d-9)((E_2(q))^2 \right. \\ &\quad \left. + 24(d-3)E_4(q) + (d^2 - 2d - 4)(E_2(\sqrt{q}))^2 + 4d(d-3)E_2(\sqrt{q})E_2(q) \right] \\ &= \frac{(4d^2 - 20d + 23)l_s^2}{24\pi R^2 (\ln \tilde{q})} + \frac{l_s^2}{144\pi R^2} \left[(d-3)(2d-9)E_2(\tilde{q}) \right. \\ &\quad \left. + 2(2d^2 - 5d - 4)E_2(\tilde{q}^2) \right] + \frac{l_s^2}{3456\pi R^2} (\ln \tilde{q}) \left[8(d+2)E_4(\tilde{q}^2) \right. \\ &\quad \left. + 6(d-3)E_4(\tilde{q}) + 4(d^2 - 2d - 4)(E_2(\tilde{q}^2))^2 \right. \\ &\quad \left. + (d-3)(d-9)(E_2(\tilde{q}))^2 + 4d(d-3)E_2(\tilde{q})E_2(\tilde{q}^2) \right] . \end{aligned} \quad (4.2)$$

See also equations (C.11), (C.18), (C.23), and (C.24). In equation (4.2), we present two equivalent expressions for the regularized nonlinear correction $\langle S_{\text{strings}}^{(2)} \rangle$, written in terms of $q = \exp(-2\pi^2 R/L)$ and $\tilde{q} = \exp(-2L/R)$, respectively. These two expressions are mapped into each other by the modular transformation (A.5), and they agree with the open-closed duality: In the open channel, equation (4.2) represents subleading corrections to the probe baryon energy levels E_{baryon} . After weighting by the Boltzmann factor $\exp(-\beta E_{\text{baryon}})$, these corrections scale with positive powers of $\ln q \sim \beta$. On the other hand, equation (4.2) splits into terms that scale as $(\ln \tilde{q})^{-1}$, $(\ln \tilde{q})^0$ and $(\ln \tilde{q})^1$ in the dual variable. As we will show shortly, the $(\ln \tilde{q})^0$ term in (4.2) encodes corrections to the local interaction vertices $C_{abc}^{(0)}$ in the closed channel, whereas the $(\ln \tilde{q})^{-1}$ and $(\ln \tilde{q})^1$ terms follow from the tree-level Feynman integral (3.20).

The kinetic action of the baryon junction (2.24) generates the following nonlinear cor-

rections at order 2:

$$\begin{aligned}
\langle (S_{\text{junction}}^{(1)})^2 \rangle &= \frac{(d+6)M^2 l_s^4}{216L^2} (\ln q) \left[2E_2(q) - E_2(\sqrt{q}) \right] + \frac{M^2 l_s^4}{20736L^2} (\ln q)^2 \\
&\quad \times \left[2(d+6)E_4(\sqrt{q}) - 8(d+6)E_4(q) + (d-2)(d+4)(E_2(\sqrt{q}))^2 \right. \\
&\quad \left. - 4(d+2)^2 E_2(\sqrt{q})E_2(q) + 4(d^2+6d+16)(E_2(q))^2 \right] \quad (4.3) \\
&= \frac{M^2 l_s^4}{1296R^2} \left[8(d+6)E_4(\tilde{q}^2) - 2(d+6)E_4(\tilde{q}) - 4(d+2)^2 E_2(\tilde{q})E_2(\tilde{q}^2) \right. \\
&\quad \left. + (d^2+6d+16)(E_2(\tilde{q}))^2 + 4(d-2)(d+4)(E_2(\tilde{q}^2))^2 \right].
\end{aligned}$$

See also equations (C.12), (C.25), and (C.28). Equation (4.3) scales as $(\ln \tilde{q})^0$ in the variable \tilde{q} , indicating that the baryon junction mass M affects only the local interaction vertices in the effective action (2.12). We will return to this point in Section 4.2.

Finally, the longitudinal displacements (2.27) gives rise to the nonlinear correction

$$\begin{aligned}
\langle (S_{\text{displacement}}^{(1)})^2 \rangle &= \frac{\pi l_s^2}{1728L^2} (\ln q) \\
&\quad \times \left[(E_2(\sqrt{q}))^2 + 4(d-3)(E_2(q))^2 - E_4(\sqrt{q}) - 4(d-3)E_4(q) \right] \quad (4.4) \\
&= \frac{(d-2)l_s^2}{3\pi R^2} (\ln \tilde{q}) + \frac{l_s^2}{18\pi R^2} \left[(d-3)E_2(\tilde{q}) + 2E_2(\tilde{q}^2) \right] + \frac{l_s^2}{432\pi R^2} (\ln \tilde{q}) \\
&\quad \times \left[4(E_2(\tilde{q}^2))^2 + (d-3)(E_2(\tilde{q}))^2 - (d-3)E_4(\tilde{q}) - 4E_4(\tilde{q}^2) \right].
\end{aligned}$$

See equation (C.13), (C.30), (C.32) and (C.34). Notably, equation (4.4) contains contributions scaling as $(\ln \tilde{q})^{-1}$, $(\ln \tilde{q})^0$ and $(\ln \tilde{q})^1$ when written in terms of the variable \tilde{q} , which differs from the corrections on the baryon junction worldline $\langle S_{\text{junction}}^{(1)} \rangle$ and $\langle (S_{\text{junction}}^{(1)})^2 \rangle$.

4.2 Saddle-point approximation

In Section 3.2, we argued that the baryon partition function (3.5) can be evaluated by the tree-level Feynman integral (3.20), which describes the s -wave scattering in the closed channel. We now compute the integral via the saddle-point approximation and include the nonlinear corrections at order 2.

The saddle point is given by the d -dimensional vector $\vec{W} = (W_1, W_2, \dots)$ that maximizes the integrand of equation (3.20). Finding such a vector reduces to the Fermat–Weber problem, which we solve perturbatively in powers of $R^{-1} \sim \beta^{-1}$. Denoting the energy levels of the closed string states in (2.4) by n_a , n_b , and n_c , we find that

$$\vec{W}_{\text{saddle}} = \frac{Ll_s^2}{3\pi R^2} (2n_a - n_b - n_c, \sqrt{3}(n_b - n_c), 0, \dots) + O(R^{-3}). \quad (4.5)$$

Around the saddle point (4.5), the s -wave scattering amplitude (3.20) reduces to a Gaussian integral. It is convenient to introduce $\vec{W} = \vec{W}_{\text{saddle}} + \delta\vec{W}$, such that the partition function

takes the form

$$\mathcal{Z} = \sum_{a,b,c} C_{abc}^{(0)} v_a v_b v_c F_{abc} l_s^{-d} \int d^d \vec{W} \exp(-\lambda_{ij} \delta W_i \delta W_j) \times \left(1 - \lambda_{ijkl} \delta W_i \delta W_j \delta W_k \delta W_l + \frac{1}{2} (\lambda_{ijk} \delta W_i \delta W_j \delta W_k)^2 + O(\partial^4) \right), \quad (4.6)$$

where $1 \leq i, j, k, l \leq d$. In equation (4.6), F_{abc} denotes the maximum of the integrand (3.20) (i.e., the saddle point value), and it reads

$$F_{abc} = \left(\frac{3}{2\pi} \right)^{\frac{d}{2}} \left(\frac{\pi R}{L} \right)^{\frac{3}{2}(d-1)} \frac{e^{-6\pi RL/l_s^2}}{2\tilde{q}^{\frac{d-1}{8}}} \tilde{q}^{n_a+n_b+n_c} \left\{ 1 - \frac{l_s^2}{2\pi R^2} \left[\frac{3(d-3)(d-1)}{4 \ln \tilde{q}} + \frac{(d-1)}{8} (d-1-8(n_a+n_b+n_c)) + \left(\frac{(d-1)^2}{64} - \frac{(d-1)}{4} (n_a+n_b+n_c) + 6(n_a^2+n_b^2+n_c^2) - (n_a+n_b+n_c)^2 \right) \frac{\ln \tilde{q}}{3} \right] + O(\partial^4) \right\}. \quad (4.7)$$

The coefficients λ_{ij} , λ_{ijk} , and λ_{ijkl} are fully symmetric in the spatial indices, and the non-zero coefficients are listed in table 1.

	$\lambda \times \left(-\frac{\ln \tilde{q}}{3\pi}\right)$		$\lambda \times \left(-\frac{\ln \tilde{q}}{3\pi}\right)$
		λ_{111}	$\frac{1}{(\ln \tilde{q}) l_s^2 R}$
λ_{11}	$\frac{1}{l_s^2} + (n_b + n_c - n_a - \frac{d-1}{24}) \frac{1}{\pi R^2}$	λ_{122}	$-\frac{1}{(\ln \tilde{q}) l_s^2 R}$
λ_{22}	$\frac{1}{l_s^2} + (\frac{5}{3}n_a - \frac{1}{3}n_b - \frac{1}{3}n_c - \frac{d-1}{24}) \frac{1}{\pi R^2}$	$\lambda_{1111}, \lambda_{2222}$	$\frac{1}{4(\ln \tilde{q})^2 l_s^2 R^2}$
λ_{12}	$(n_b - n_c) \frac{2}{\sqrt{3}\pi R^2}$	λ_{1122}	$\frac{1}{12(\ln \tilde{q})^2 l_s^2 R^2}$
λ_{jj}	$\frac{2}{l_s^2} + (\frac{2}{3}(n_a + n_b + n_c) - \frac{d-1}{12} - \frac{d-1}{\ln \tilde{q}}) \frac{1}{\pi R^2}$	$\lambda_{11jj}, \lambda_{22jj}$	$\frac{1}{3(\ln \tilde{q})^2 l_s^2 R^2}$
		λ_{jjjj}	$-\frac{2}{(\ln \tilde{q})^2 l_s^2 R^2}$
		$\lambda_{jjkk} (j \neq k)$	$-\frac{2}{3(\ln \tilde{q})^2 l_s^2 R^2}$

Table 1: Saddle point coefficients of the Feynman integral. In this table, we take $3 \leq j, k \leq d$. The coefficients are given in units of $(-\frac{\ln \tilde{q}}{3\pi}) = \frac{2L}{3\pi R}$, and we retain terms up to the order $O(\partial^2)$.

Carrying out the Gaussian integral (4.6), we find that

$$\mathcal{Z} = \left(\frac{\pi R}{L} \right)^{d-\frac{3}{2}} \frac{e^{-6\pi RL/l_s^2}}{2^{\frac{d}{2}} \tilde{q}^{\frac{d-1}{8}}} \sum_{a,b,c} C_{abc}^{(0)} v_a v_b v_c \tilde{q}^{n_a+n_b+n_c} \left\{ 1 - \frac{l_s^2}{6\pi R^2} \left[\frac{4d^2 - 24d + 31}{4 \ln \tilde{q}} + \frac{(2d-3)}{8} (d-1-8(n_a+n_b+n_c)) + \left(\frac{(d-1)^2}{64} - \frac{d-1}{4} (n_a+n_b+n_c) + 6(n_a^2+n_b^2+n_c^2) - (n_a+n_b+n_c)^2 \right) \ln \tilde{q} \right] + O(\partial^4) \right\}. \quad (4.8)$$

Notably, the locality of the interaction vertices in (3.18) requires the coupling constants $C_{abc}^{(0)}$ to be independent of the confining string length $L \sim \ln \tilde{q}$. For the open-closed duality to be consistent, the terms scaling as $(\ln \tilde{q})^1$ and $(\ln \tilde{q})^{-1}$ in equation (4.8) must match exactly with those obtained from the open-channel calculation. That is indeed the case.

To make a direct comparison, we collect the expansion in \tilde{q} of the results (3.17), (4.1), (4.2), (4.3), and (4.4) as follows

$$\begin{aligned}
\mathcal{Z}^{(0)} &= \left(\frac{\pi R}{L}\right)^{d-\frac{3}{2}} \frac{1}{2^{\frac{d}{2}} \tilde{q}^{\frac{d-1}{8}}} (1 + (d-3)\tilde{q} + O(\tilde{q}^2)) ; \\
\langle S_{\text{junction}}^{(1)} \rangle &= -\frac{(2+d)Ml_s^2}{36R} (1 + 24\tilde{q} + O(\tilde{q}^2)) ; \\
\langle S_{\text{strings}}^{(2)} \rangle &= \frac{l_s^2}{\pi R^2} \left[\left(\frac{4d^2 - 20d + 23}{24(\ln \tilde{q})} + \frac{6d^2 - 25d + 19}{144} + \frac{(d-1)^2}{384} (\ln \tilde{q}) \right) \right. \\
&\quad \left. + \left(-\frac{2d^2 - 15d + 27}{6} - \frac{(d^2 - 16d + 39)}{24} (\ln \tilde{q}) \right) \tilde{q} + O(\tilde{q}^2) \right] ; \\
\langle (S_{\text{junction}}^{(1)})^2 \rangle &= \frac{M^2 l_s^4}{R^2} \left(\frac{(d+2)^2}{1296} + \frac{d^2 - 8d - 68}{27} \tilde{q} + O(\tilde{q}^2) \right) ; \\
\langle (S_{\text{displacement}}^{(1)})^2 \rangle &= \frac{l_s^2}{\pi R^2} \left(\frac{d-2}{3(\ln \tilde{q})} + \frac{d-1}{18} - \frac{2(d-3)}{3} (2 + \ln \tilde{q}) \tilde{q} + O(\tilde{q}^2) \right) .
\end{aligned} \tag{4.9}$$

Matching the closed-channel scattering amplitudes (4.8) with the open-channel partition function (4.9), we obtain the following two cubic coupling constants:

$$\begin{aligned}
C_{\mathbf{000}}^{(0)} &= e^{-2\pi RM} \left[1 + \frac{(d+2)Ml_s^2}{36R} + \frac{5(d-1)l_s^2}{144\pi R^2} + \frac{(d+2)^2 M^2 l_s^4}{2592R^2} + O(R^{-3}) \right] , \\
C_{\mathbf{001}}^{(0)} &= \frac{e^{-2\pi RM}}{3\sqrt{d-1}} \left[(d-3) + \frac{(d+2)(d+21)Ml_s^2}{36R} + \frac{(d-3)(5d-173)l_s^2}{144\pi R^2} \right. \\
&\quad \left. + \frac{(d^3 + 49d^2 - 392d - 3276)M^2 l_s^4}{2592R^2} + O(R^{-3}) \right] ,
\end{aligned} \tag{4.10}$$

which are independent of $L \sim \ln \tilde{q}$. In particular, we note that $C_{\mathbf{001}}^{(0)} = O(R^{-3})$ when $d = 3$ and $M = 0$. This agrees with the selection rule (3.31) that follows from the \mathbb{Z}_2 symmetry (3.25) of the low-energy effective theory.

5 Ground state energies of probe baryons

In this section, we use the effective field theory (2.16) to make predictions for baryons that can be tested in lattice simulations. In particular, we focus on the ground state energies of the probe baryons shown in figure 1. When the baryon is treated as a point-like particle at long distances, the ground state energy is also referred to as the static mass of the baryon. See, e.g., [20, 21, 28, 75, 76] and references therein for numerical studies on this subject.

The ground state energy E_{GS} is dominated by the classical contributions from the effective actions (2.17) and (2.23). We find that

$$E_{\text{GS}} = \frac{L_x + L_y + L_z}{l_s^2} + M + E_{\text{GS}}^{(0)} + O(\partial^2) , \tag{5.1}$$

where $E_{\text{GS}}^{(0)}$ denotes the leading correction from quantum fluctuations. Since the order 0 effective action is entirely fixed by $S_{\text{strings}}^{(0)}$ in equation (2.18), the leading correction $E_{\text{GS}}^{(0)} = E_{\text{GS}}^{(0)}(L_x, L_y, L_z)$ is independent of both the string tension l_s^{-2} and the junction mass M . While a closed form for $E_{\text{GS}}^{(0)}$ is not readily available, we note that it can be obtained from the open channel partition function (3.13) when the ratios of L_x, L_y, L_z are rational. We refer to equation (B.9) and the discussion in Appendix B for further details. A few results of equation (B.9) are listed in table 2.

$L_x : L_y : L_z$	$E_{\text{GS}}^{(0)} \times \min(L_x, L_y, L_z)$
1 : 1 : 2	$\approx -0.159d + 0.323$
1 : 1 : 3	$\approx -0.144d + 0.298$
1 : 3 : 6	$\approx -0.083d + 0.179$
2 : 3 : 5	$\approx -0.130d + 0.265$

Table 2: Leading quantum corrections to the ground-state energy of probe baryons. In this table, we present $E_{\text{GS}}^{(0)}$ for probe baryons at rational points (see Appendix B). The coefficients are displayed to three decimal places.

We now turn to special baryon configurations, starting with

$$\text{isosceles baryon : } L_x = L_1, L_y = L_z = L_2. \quad (5.2)$$

In particular, we consider the two limits $L_1 \ll L_2$ and $L_1 \gg L_2$. See also figure 6. In either limit, the quantum fluctuations on the short and the long strings are associated with two widely separated scales. For isosceles baryons with $L_1 \ll L_2$, we find that

$$E_{\text{GS}}^{(0)} = -\frac{(d-2)\text{Li}_2\left(\frac{1}{3}\right) + \text{Li}_2\left(-\frac{1}{3}\right)}{4\pi L_1} + O(L_2^{-1}). \quad (5.3)$$

We interpret this as the correction to the ground state energy of a single confining string stretching between a static quark and the baryon junction. On the other hand, we find that for isosceles baryons with $L_1 \gg L_2$:

$$E_{\text{GS}}^{(0)} = -\frac{(2d-5)\pi}{48L_2} - \frac{(d-2)\text{Li}_2\left(-\frac{1}{3}\right) + \text{Li}_2\left(\frac{1}{3}\right)}{4\pi L_2} + O(L_1^{-1}). \quad (5.4)$$

For the equilateral baryons in equation (3.16), the ground-state energy can be analyzed more explicitly. This energy can be computed using the open-channel representation of the partition function (3.5), with contributions given in equations (3.17), (4.1), (4.2), (4.3), and (4.4). We organize these contributions in an expansion of the modular parameter

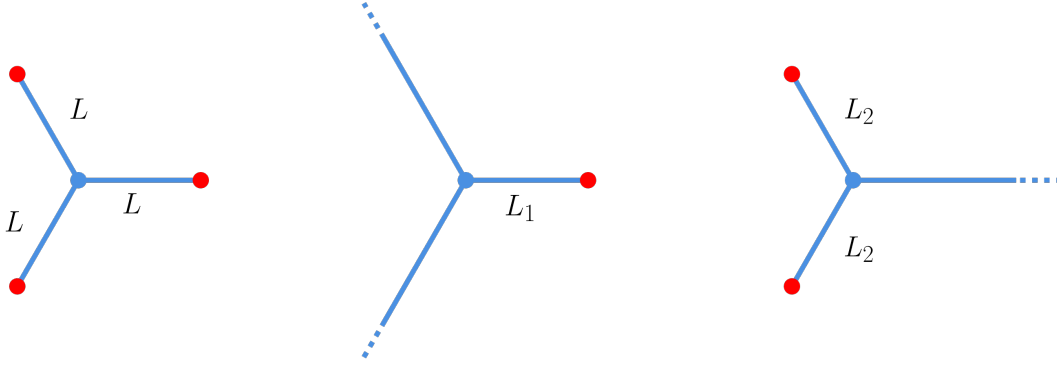


Figure 6: Different limits of the probe baryon configuration. Left: the equilateral baryon; Middle: the isosceles baryon with $L_1 \ll L_2$; Right: the isosceles baryon with $L_1 \gg L_2$. In the middle and right panels, the long strings are taken to extend to spatial infinity.

$q = \exp(-\pi\beta/L)$ as follows:

$$\begin{aligned}
\mathcal{Z}^{(0)} &= q^{\frac{2-d}{16}} \left[1 + d\sqrt{q} + O(q) \right] ; \\
\langle S_{\text{junction}}^{(1)} \rangle &= \frac{Ml_s^2}{L} (\ln q) \left[\frac{d+2}{144} + \frac{d+2}{6} \sqrt{q} + O(q) \right] ; \\
\langle S_{\text{strings}}^{(2)} \rangle &= \frac{l_s^2}{L^2} (\ln q) \left[\frac{\pi(d-2)^2}{1536} - \frac{\pi(d^2-6d-8)}{96} \sqrt{q} + O(q) \right] ; \\
\langle (S_{\text{junction}}^{(1)})^2 \rangle &= \frac{M^2 l_s^4}{L^2} (\ln q) \left[\frac{d+6}{216} + \frac{d+6}{9} \sqrt{q} + O(q) \right] \\
&\quad + \frac{M^2 l_s^4}{L^2} (\ln q)^2 \left[\frac{(d+2)^2}{20736} + \frac{(d^2+16d+76)}{432} \sqrt{q} + O(q) \right] ; \\
\langle (S_{\text{displacement}}^{(1)})^2 \rangle &= \frac{l_s^2}{L^2} (\ln q) \left[-\frac{\pi}{6} \sqrt{q} + O(q) \right] .
\end{aligned} \tag{5.5}$$

Comparing the leading terms in the expansion (5.5) with the Boltzmann weight $\exp(-\beta E_{\text{GS}})$ yields the ground state energy:

$$\begin{aligned}
E_{\text{GS}} &= \frac{3L}{l_s^2} + M - \frac{(d-2)\pi}{16L} - \frac{(d+2)\pi M l_s^2}{144L^2} \\
&\quad + \frac{(d+6)\pi M^2 l_s^2}{432L^3} - \frac{(d-2)^2 \pi^2 l_s^2}{1536L^3} + O(L^{-4}) .
\end{aligned} \tag{5.6}$$

Notably, the quantum corrections in (5.6) are fixed by the two classical parameters (i.e., the string tension l_s^{-2} and the junction mass M) up to the next-to-next-to-leading order. This is a consequence of the Poincaré symmetry and diffeomorphism invariance on the confining string worldsheet. In lattice simulations [76], the junction mass M is extracted by fitting the L^{-2} term in (5.6). The new L^{-3} result should improve fit precision and deepen our understanding of confinement.

Acknowledgments

We are especially grateful to Zohar Komargodski for many stimulating and helpful discussions on this project. We thank Arkya Chatterjee, Gabriel Cuomo, Leonardo Rastelli, Shu-Heng Shao, and Yunqin Zheng for interesting discussions. We also thank Jan Albert and Zohar Komargodski for thoughtful comments on the draft. XL and SZ are supported in part by the Simons Foundation grant 488657 (Simons Collaboration on the Non-Perturbative Bootstrap), the BSF grant no. 2018204 and NSF award number 2310283. The authors of this paper are ordered alphabetically.

A Modular functions

In this appendix, we collect definitions and properties of modular functions that we have used in the main text. The Dedekind eta function is defined by

$$\eta(q) \equiv q^{\frac{1}{24}} \prod_{n \in \mathbb{N}^+} (1 - q^n) . \quad (\text{A.1})$$

The Eisenstein series is defined by

$$E_{2k}(q) \equiv 1 + \frac{2}{\zeta(1-2k)} \sum_{n \in \mathbb{N}^+} \frac{n^{2k-1} q^n}{1 - q^n} , \quad (\text{A.2})$$

where $\zeta(s)$ is the Riemann zeta function. Finally, the infinite product representation of the odd Jacobi theta function is as follows:

$$\vartheta_1(u; q) \equiv 2q^{\frac{1}{8}} \sin(\pi u) \prod_{n \in \mathbb{N}^+} (1 - q^n)(e^{2\pi i u} - q^n)(e^{-2\pi i u} - q^n) . \quad (\text{A.3})$$

Throughout this paper, we adopt the convention that the modular parameter $q = e^{2\pi i \tau}$ and the dual parameter $\tilde{q} = e^{2\pi i \tilde{\tau}}$, with $\tilde{\tau} = -1/\tau$. The functions (A.1) and (A.3) are known to satisfy the following modular identities:

$$\begin{aligned} \eta(q) &= \sqrt{-i\tilde{\tau}} \eta(\tilde{q}) , \\ \vartheta_1(u; q) &= -i\sqrt{-i\tilde{\tau}} \exp(\pi i u^2 \tilde{\tau}) \vartheta_{11}(u\tilde{\tau}; \tilde{q}) . \end{aligned} \quad (\text{A.4})$$

As far as the discussion in the main text is concerned, we also note the following two identities of Eisenstein series E_2 and E_4 :

$$\begin{aligned} E_2(q) &= -\frac{6i}{\pi} \tilde{\tau} + \tilde{\tau}^2 E_2(\tilde{q}) , \\ E_4(q) &= \tilde{\tau}^4 E_4(\tilde{q}) . \end{aligned} \quad (\text{A.5})$$

B Probe baryons at rational points

In this appendix, we discuss special configurations of the probe baryon in figure 1. We focus on the cases where the ratios of the three confining string lengths are rational:

$$\begin{aligned} \text{rational points} : \quad & L_x = N_x L , \quad L_y = N_y L , \quad L_z = N_z L , \\ & \text{s.t. } N_x, N_y, N_z \in \mathbb{N}^+ \quad \text{and} \quad \text{gcd}(N_x, N_y, N_z) = 1 . \end{aligned} \quad (\text{B.1})$$

Let us first note several useful mathematical facts concerning N_x , N_y , and N_z . In particular, consider the following two polynomials:

$$\begin{aligned} P_1(r) &\equiv 1 + \frac{1}{3}(r^{N_x} + r^{N_y} + r^{N_z}) - \frac{1}{3}(r^{N_x+N_y} + r^{N_y+N_z} + r^{N_z+N_x}) - r^{N_x+N_y+N_z}, \\ P_2(r) &\equiv 1 - \frac{1}{3}(r^{N_x} + r^{N_y} + r^{N_z}) - \frac{1}{3}(r^{N_x+N_y} + r^{N_y+N_z} + r^{N_z+N_x}) + r^{N_x+N_y+N_z}. \end{aligned} \quad (\text{B.2})$$

Both $P_1(r)$ and $P_2(r)$ have all of their roots on the unit circle $|r| = 1$ [77]. We can therefore write the factorization

$$P_1(r) = (1-r) \prod_u (e^{2\pi i u} - r), \quad P_2(r) = (1-r)^2 \prod_v (e^{2\pi i v} - r), \quad (\text{B.3})$$

where $0 < u < 1$ denotes the phases of the $(N_x + N_y + N_z - 1)$ non-identity roots of P_1 , and $0 < v < 1$ denotes the phases of the $(N_x + N_y + N_z - 2)$ non-identity roots of P_2 . These phases are subject to the following conditions

$$\begin{aligned} \prod_u (2 \sin(\pi u)) &= \frac{4}{3}(N_x + N_y + N_z), \\ \prod_v (2 \sin(\pi v)) &= \frac{2}{3}(N_x N_y + N_y N_z + N_z N_x). \end{aligned} \quad (\text{B.4})$$

We now turn to the baryon partition function (3.13) at the rational points (B.2). Adopting the notation $q = \exp(-2\pi^2 R/L)$ and $\tilde{q} = \exp(-2L/R)$ as in the previous sections, we find that

$$\begin{aligned} &\prod_{n \in \mathbb{N}^+} \frac{\tanh(\frac{nN_x L}{R}) + \tanh(\frac{nN_y L}{R}) + \tanh(\frac{nN_z L}{R})}{\tanh(\frac{nN_x L}{R}) \tanh(\frac{nN_y L}{R}) \tanh(\frac{nN_z L}{R})} \\ &= \prod_{n \in \mathbb{N}^+} \frac{3P_1(\tilde{q}^n)}{(1 - \tilde{q}^{nN_x})(1 - \tilde{q}^{nN_y})(1 - \tilde{q}^{nN_z})} \\ &= \frac{L}{2\pi R} \sqrt{\frac{N_x N_y N_z}{N_x + N_y + N_z}} \frac{\eta(q)}{\eta(q^{\frac{1}{N_x}}) \eta(q^{\frac{1}{N_y}}) \eta(q^{\frac{1}{N_z}})} \left(\prod_u q^{\frac{(u-\frac{1}{2})^2}{4} - \frac{1}{48}}(q^u; q)_\infty \right), \end{aligned} \quad (\text{B.5})$$

where we have used the q -Pochhammer symbol. Similarly,

$$\begin{aligned} &\prod_{n \in \mathbb{N}^+} \left(\coth(\frac{nN_x L}{R}) + \coth(\frac{nN_y L}{R}) + \coth(\frac{nN_z L}{R}) \right) \\ &= \prod_{n \in \mathbb{N}^+} \frac{3P_2(\tilde{q}^n)}{(1 - \tilde{q}^{nN_x})(1 - \tilde{q}^{nN_y})(1 - \tilde{q}^{nN_z})} \\ &= \frac{1}{\sqrt{2\pi R(N_x^{-1} + N_y^{-1} + N_z^{-1})}} \frac{(\eta(q))^2}{\eta(q^{\frac{1}{N_x}}) \eta(q^{\frac{1}{N_y}}) \eta(q^{\frac{1}{N_z}})} \left(\prod_v q^{\frac{(v-\frac{1}{2})^2}{4} - \frac{1}{48}}(q^v; q)_\infty \right). \end{aligned} \quad (\text{B.6})$$

In equations (B.5) and (B.6), we have used the fact that both P_1 and P_2 are real polynomials, as well as the modular identity that follows from equation (A.4):

$$\tilde{q}^{\frac{1}{24}} \prod_{n \in \mathbb{N}^+} (e^{2\pi i n \alpha} - \tilde{q}^n)(e^{-2\pi i n \alpha} - \tilde{q}^n) = \frac{q^{\frac{1}{2}(\alpha - \frac{1}{2})^2 - \frac{1}{24}}}{2 \sin(\pi \alpha)} (q^\alpha; q)_\infty (q^{1-\alpha}; q)_\infty. \quad (\text{B.7})$$

In terms of the roots of P_1 and P_2 , we find that the baryon partition function (3.13) takes the form

$$\mathcal{Z}^{(0)} = \frac{1}{(\eta(q))^{2d-3}} \left(\prod_u \frac{q^{\frac{1}{48} - \frac{(u-\frac{1}{2})^2}{4}}}{(q^u; q)_\infty} \right) \left(\prod_v \frac{q^{\frac{1}{48} - \frac{(v-\frac{1}{2})^2}{4}}}{(q^v; q)_\infty} \right)^{d-2}. \quad (\text{B.8})$$

This partition function (B.8) indicates that the probe baryon system in the open channel (3.1) has a unique ground state. Moreover, we find the leading quantum correction to the ground state energy (5.1):

$$E_{\text{GS}}^{(0)} = -\frac{(2d-3)\pi}{24L} - \frac{\pi}{4L} \sum_u \left(\left(u - \frac{1}{2}\right)^2 - \frac{1}{12} \right) - \frac{(d-2)\pi}{4L} \sum_v \left(\left(v - \frac{1}{2}\right)^2 - \frac{1}{12} \right). \quad (\text{B.9})$$

Next, we analyze various limits of the probe baryon configurations introduced in sections 3 and 5. For the equilateral baryon with $N_x = N_y = N_z = 1$, we obtain

$$\text{equilateral baryon : } u_1 = u_2 = v_1 = \frac{1}{2}, \quad (\text{B.10})$$

in which case equation (B.8) is reduced to equation (3.17).

For isosceles baryons, we first consider $N_x = 1$ and $N_y = N_z = N \gg 1$, corresponding to the $L_1 \ll L_2$ baryon configuration in equation (5.3). See also figure 6. In this case, both polynomials P_1 and P_2 admit two branches of nontrivial roots, with the first exact branch given by

$$\begin{aligned} \text{isosceles baryons } L_1 \ll L_2 : \quad u_k^{(1)} &= \frac{1}{N} \left(k - \frac{1}{2}\right), \quad \text{for } 1 \leq k \leq N; \\ v_k^{(1)} &= \frac{k}{N}, \quad \text{for } 1 \leq k \leq N-1. \end{aligned} \quad (\text{B.11})$$

The remaining roots of P_1 and P_2 are algebraic, but they cannot be written in closed form for generic N . We can solve them perturbatively in the limit $N \gg 1$:

isosceles baryons $L_1 \ll L_2$:

$$\begin{aligned} u_k^{(2)} &= \frac{k}{N+1} + \frac{1}{N+1} f^+\left(\frac{k}{N+1}\right) + O(N^{-2}), \quad \text{for } 1 \leq k \leq N; \\ v_k^{(2)} &= \frac{k}{N+1} + \frac{1}{N+1} f^-\left(\frac{k}{N+1}\right) + O(N^{-2}), \quad \text{for } 1 \leq k \leq N, \end{aligned} \quad (\text{B.12})$$

so that these roots are almost uniformly distributed on the unit circle. In equation (B.12), we have introduced the function

$$f^\pm(\alpha) \equiv \alpha + \frac{1}{2\pi} \arg \left(\frac{3 \pm e^{2\pi i \alpha}}{3e^{2\pi i \alpha} \pm 1} \right), \quad \text{where } 0 \leq \arg < 2\pi. \quad (\text{B.13})$$

Using the roots in equations (B.11) and (B.12), we find the ground state energy (B.9)

$$E_{\text{GS}}^{(0)} = -\frac{\pi}{4L} \int_0^1 d\alpha (2\alpha - 1) (f^+(\alpha) + (d-2)f^-(\alpha)) + O(N^{-1}), \quad (\text{B.14})$$

which evaluates to equation (5.3).

We next consider $N_x = N \gg 1$ and $N_y = N_z = 1$, corresponding to the $L_1 \gg L_2$ baryon configuration in equation (5.4). See also figure 6. The non-trivial roots of the polynomial P_1 in this case take the form:

$$\begin{aligned} \text{isosceles baryons } L_1 \gg L_2 : \quad u^{(1)} &= \frac{1}{2}; \\ u_k^{(2)} &= \frac{k}{N+1} + \frac{1}{N+1} f^-\left(\frac{k}{N+1}\right) + O(N^{-2}), \quad \text{for } 1 \leq k \leq N. \end{aligned} \quad (\text{B.15})$$

On the other hand, the corresponding roots of the polynomial P_2 are given by

$$\text{isosceles baryons } L_1 \gg L_2 : \quad v_k = \frac{k}{N+1} + \frac{1}{N+1} f^+\left(\frac{k}{N+1}\right) + O(N^{-2}), \quad \text{for } 1 \leq k \leq N. \quad (\text{B.16})$$

We thus find that the ground state energy (B.9) yields equation (5.4):

$$E_{\text{GS}}^{(0)} = -\frac{(2d-5)\pi}{48L} - \frac{\pi}{4L} \int_0^1 d\alpha (2\alpha-1) ((d-2)f^+(\alpha) + f^-(\alpha)) + O(N^{-1}). \quad (\text{B.17})$$

C Green's functions on a cylinder

This appendix collects the technical details of Green's functions and zeta-function regularization used in sections 3.1 and 4.1.

We consider a Euclidean cylinder with coordinates (τ, σ) , where $\tau \sim \tau + 2\pi R$ and $0 \leq \sigma \leq L$. The Green's functions on the cylinder are defined as the solutions to the Poisson equation:

$$(-\partial_{\tau_1}^2 - \partial_{\sigma_1}^2)G(\sigma_1, \sigma_2, \tau_{12}) = \delta(\tau_{12})\delta(\sigma_{12}), \quad (\text{C.1})$$

where $\tau_{ab} \equiv \tau_a - \tau_b$ and $\sigma_{ab} \equiv \sigma_a - \sigma_b$. We denote the Green's function with Dirichlet boundary conditions at $\sigma = 0$ and $\sigma = L$ by

$$G(\sigma_1, \sigma_2, \tau_{12}; q) = \frac{1}{\pi RL} \sum_{n \in \mathbb{N}^+} \sum_{m \in \mathbb{Z}} \frac{\sin\left(\frac{n\pi\sigma_1}{L}\right) \sin\left(\frac{n\pi\sigma_2}{L}\right) e^{i\frac{m}{R}\tau_{12}}}{\frac{\pi^2 n^2}{L^2} + \frac{m^2}{R^2}}, \quad (\text{C.2})$$

where $q = \exp(-2\pi^2 R/L)$ is the modular parameter. On the other hand, the Green's function with Neumann boundary condition at $\sigma = 0$ and Dirichlet boundary condition at $\sigma = L$ takes the form

$$\tilde{G}(\sigma_1, \sigma_2, \tau_{12}; q) = \frac{1}{\pi RL} \sum_{r \in \mathbb{N} + \frac{1}{2}} \sum_{m \in \mathbb{Z}} \frac{\cos\left(\frac{r\pi\sigma_1}{L}\right) \cos\left(\frac{r\pi\sigma_2}{L}\right) e^{i\frac{m}{R}\tau_{12}}}{\frac{\pi^2 r^2}{L^2} + \frac{m^2}{R^2}}. \quad (\text{C.3})$$

In section 3.1, we use the Dirichlet-Dirichlet Green's function (C.2) to compute the saddle-point action in equation (3.12). It is convenient to define

$$K(\tau; q) \equiv \frac{R}{L} + 2 \sum_{n \in \mathbb{N}^+} n \cos\left(\frac{n\tau}{R}\right) \coth\left(\frac{nL}{R}\right), \quad (\text{C.4})$$

such that the saddle point action $S_{\text{strings}}^{(0)}(x_i^*, y_i^*, z_i^*)$ can be written compactly as:

$$\begin{aligned}
S_{\text{strings}}^{(0)}(x_i^*, y_i^*, z_i^*) = & - \int \frac{d\tau_1 d\tau_2}{4\pi R^2} \left[\frac{3}{4} \left(K(\tau_{12}; q_y) + K(\tau_{12}; q_z) \right) w_1(\tau_1) w_1(\tau_2) \right. \\
& + \frac{\sqrt{3}}{2} \left(K(\tau_{12}; q_y) - K(\tau_{12}; q_z) \right) w_1(\tau_1) w_2(\tau_2) \\
& + \frac{1}{4} \left(4K(\tau_{12}; q_x) + K(\tau_{12}; q_y) + K(\tau_{12}; q_z) \right) w_2(\tau_1) w_2(\tau_2) \\
& \left. + \left(K(\tau_{12}; q_x) + K(\tau_{12}; q_y) + K(\tau_{12}; q_z) \right) w_j(\tau_1) w_j(\tau_2) \right]. \tag{C.5}
\end{aligned}$$

Using the Gaussian integral determinant of (C.5), we find the partition function (3.13).

In the following, we focus on the calculations of nonlinear corrections presented in section 4.1.

C.1 Wick contraction

For the equilateral baryon configuration (3.16), the free theory correlation functions between the NGB fields x_i , y_i , and z_i are given by linear combinations of the Green's functions (C.2) and (C.3). In particular, we find the propagators of the quantum fluctuations in the confining string plane:

$$\begin{aligned}
\langle x_2(\tau_1, \sigma_1) x_2(\tau_2, \sigma_2) \rangle &= \langle y_2(\tau_1, \sigma_2) y_2(\tau_2, \sigma_2) \rangle = \langle z_2(\tau_1, \sigma_2) z_2(\tau_2, \sigma_2) \rangle \\
&= \frac{1}{3} G(\sigma_1, \sigma_2, \tau_{12}; q) + \frac{2}{3} \tilde{G}(\sigma_1, \sigma_2, \tau_{12}; q), \\
\langle x_2(\tau_1, \sigma_1) y_2(\tau_2, \sigma_2) \rangle &= \langle y_2(\tau_1, \sigma_2) z_2(\tau_2, \sigma_2) \rangle = \langle z_2(\tau_1, \sigma_2) x_2(\tau_2, \sigma_2) \rangle \\
&= \frac{1}{3} G(\sigma_1, \sigma_2, \tau_{12}; q) - \frac{1}{3} \tilde{G}(\sigma_1, \sigma_2, \tau_{12}; q). \tag{C.6}
\end{aligned}$$

Similarly, we also find

$$\begin{aligned}
\langle x_j(\tau_1, \sigma_1) x_k(\tau_2, \sigma_2) \rangle &= \langle y_j(\tau_1, \sigma_1) y_k(\tau_2, \sigma_2) \rangle = \langle z_j(\tau_1, \sigma_1) z_k(\tau_2, \sigma_2) \rangle \\
&= \frac{1}{3} \delta_{jk} \tilde{G}(\sigma_1, \sigma_2, \tau_{12}; q) + \frac{2}{3} \delta_{jk} G(\sigma_1, \sigma_2, \tau_{12}; q), \\
\langle x_j(\tau_1, \sigma_1) y_k(\tau_2, \sigma_2) \rangle &= \langle y_j(\tau_1, \sigma_1) z_k(\tau_2, \sigma_2) \rangle = \langle z_j(\tau_1, \sigma_1) x_k(\tau_2, \sigma_2) \rangle \\
&= \frac{1}{3} \delta_{jk} \tilde{G}(\sigma_1, \sigma_2, \tau_{12}; q) - \frac{1}{3} \delta_{jk} G(\sigma_1, \sigma_2, \tau_{12}; q), \tag{C.7}
\end{aligned}$$

where $3 \leq j, k \leq d$ denote spatial directions perpendicular to the confining string plane. We note that the other propagators (e.g. $\langle x_2 y_j \rangle$) are identically zero.

We now use Wick's theorem to obtain the nonlinear corrections $\langle S_{\text{displacement}}^{(2)} \rangle$, $\langle S_{\text{strings}}^{(2)} \rangle$, $\langle (S_{\text{junction}}^{(1)})^2 \rangle$, and $\langle (S_{\text{displacement}}^{(1)})^2 \rangle$ for the equilateral baryon configuration. First, we find

that the quartic term at the baryon junction arising from longitudinal displacements takes the form

$$\begin{aligned} \langle S_{\text{displacement}}^{(2)} \rangle &= \frac{l_s^2}{3} \int d\tau [(2d-3)\tilde{G}(\partial_{\tau_1}\partial_{\tau_2}\partial_{\sigma_1}G + \partial_{\sigma_1}^2\partial_{\sigma_2}G) \\ &\quad + d\tilde{G}(\partial_{\tau_1}\partial_{\tau_2}\partial_{\sigma_1}\tilde{G} + \partial_{\sigma_1}^2\partial_{\sigma_2}\tilde{G})] \Big|_{\tau_{12}=0, \sigma_1=\sigma_2=0} . \end{aligned} \quad (\text{C.8})$$

It is straightforward to check that the triple derivatives of the Green's functions (C.2) and (C.3) at the coincident point $\tau_{12} = 0, \sigma_1 = \sigma_2 = 0$ satisfy

$$\partial_{\tau_1}\partial_{\tau_2}\partial_{\sigma_1}G = \partial_{\sigma_1}^2\partial_{\sigma_2}G = \partial_{\tau_1}\partial_{\tau_2}\partial_{\sigma_1}\tilde{G} = \partial_{\sigma_1}^2\partial_{\sigma_2}\tilde{G} = 0 . \quad (\text{C.9})$$

We therefore conclude $\langle S_{\text{displacement}}^{(2)} \rangle = 0$ as in equation (4.1).

For the worldsheet nonlinear correction $\langle S_{\text{strings}}^{(2)} \rangle$, we introduce the following short-handed notations

$$\begin{aligned} G_{\alpha\beta}(\sigma) &\equiv (\partial_{\alpha_1}\partial_{\beta_2}G(\sigma_1, \sigma_2, \tau_{12}; q)) \Big|_{\tau_{12}=0, \sigma_1=\sigma_2=\sigma} , \\ \tilde{G}_{\alpha\beta}(\sigma) &\equiv (\partial_{\alpha_1}\partial_{\beta_2}\tilde{G}(\sigma_1, \sigma_2, \tau_{12}; q)) \Big|_{\tau_{12}=0, \sigma_1=\sigma_2=\sigma} . \end{aligned} \quad (\text{C.10})$$

These are the double derivatives of the Green's functions in the coincident point limit. In particular, we have $G_{\tau\sigma}(\sigma) = \tilde{G}_{\tau\sigma}(\sigma) = 0$. Applying Wick's theorem to $\langle S_{\text{strings}}^{(2)} \rangle$, we obtain

$$\begin{aligned} \langle S_{\text{strings}}^{(2)} \rangle &= -\frac{l_s^2}{24} \int d\tau d\sigma [(4d^2 - 4d - 5)(G_{\sigma\sigma}^2 + G_{\tau\tau}^2) \\ &\quad - 2(4d^2 - 20d + 23)G_{\tau\tau}G_{\sigma\sigma} + (d^2 + 2d + 4)(\tilde{G}_{\sigma\sigma}^2 + \tilde{G}_{\tau\tau}^2) \\ &\quad - 2(d^2 - 2d - 4)\tilde{G}_{\tau\tau}\tilde{G}_{\sigma\sigma} + 2(2d^2 + d - 4)(G_{\sigma\sigma}\tilde{G}_{\sigma\sigma} + G_{\tau\tau}\tilde{G}_{\tau\tau}) \\ &\quad - (4d^2 - 14d + 8)(G_{\sigma\sigma}\tilde{G}_{\tau\tau} + G_{\tau\tau}\tilde{G}_{\sigma\sigma})] . \end{aligned} \quad (\text{C.11})$$

The integrals in equation (C.11) are divergent, and we evaluate them using zeta-function regularization in the following. See equations (C.18), (C.23), and (C.24).

The nonlinear correction arising from the baryon junction kinetic term reads

$$\begin{aligned} \langle (S_{\text{junction}}^{(1)})^2 \rangle &= \frac{(d+2)^2}{36} M^2 l_s^4 \int d\tau_1 d\tau_2 (\tilde{G}_{\tau\tau}^2) \Big|_{\sigma=0} \\ &\quad + \frac{d+6}{18} M^2 l_s^4 \int d\tau_1 d\tau_2 (\partial_{\tau_1}\partial_{\tau_2}\tilde{G}(\tau_{12}))^2 \Big|_{\sigma_1=\sigma_2=0} . \end{aligned} \quad (\text{C.12})$$

We refer the reader to equations (C.25) and (C.28) for the regularization of this divergent integral. Finally, the longitudinal displacements contribute the following nonlinear corrections

$$\begin{aligned} \langle (S_{\text{displacement}}^{(1)})^2 \rangle &= \frac{l_s^2}{3} \int d\tau_1 d\tau_2 [(d-2)\tilde{G}(\tau_{12})(\partial_{\sigma_1}\partial_{\sigma_2}G(\tau_{12}))^2 \\ &\quad + \tilde{G}(\tau_{12})(\partial_{\tau_1}\partial_{\tau_2}\tilde{G}(\tau_{12}))^2 - 2(\partial_{\tau_1}\tilde{G}(\tau_{12}))^2\partial_{\tau_1}\partial_{\tau_2}\tilde{G}(\tau_{12})] \Big|_{\sigma_1=\sigma_2=0} , \end{aligned} \quad (\text{C.13})$$

which we regularize in equations (C.30), (C.32) and (C.34).

C.2 Zeta-function regularization

In this section, we elaborate on the regularization scheme used in section 4.1.

For the divergent integrals in equation (C.11), we note the following infinite sums that yield Eisenstein series (A.2)

$$\begin{aligned} \sum_{n \in \mathbb{N}^+} \sum_{m \in \mathbb{Z}} \frac{\frac{\pi^2 n^2}{L^2}}{\frac{\pi^2 n^2}{L^2} + \frac{m^2}{R^2}} &= -\frac{\ln q}{2} \sum_{n \in \mathbb{N}} n \frac{1+q^n}{1-q^n} = \frac{\ln q}{24} E_2(q) , \\ \sum_{n \in \mathbb{N}^+} \sum_{m \in \mathbb{Z}} \frac{\frac{m^2}{R^2}}{\frac{\pi^2 n^2}{L^2} + \frac{m^2}{R^2}} &= -\sum_{n \in \mathbb{N}^+} \sum_{m \in \mathbb{Z}} \frac{\frac{\pi^2 n^2}{L^2}}{\frac{\pi^2 n^2}{L^2} + \frac{m^2}{R^2}} = -\frac{\ln q}{24} E_2(q) , \end{aligned} \quad (\text{C.14})$$

where we have used the zeta-function identities

$$\sum_{n \in \mathbb{N}} n^1 = \zeta(-1) = -\frac{1}{12} , \quad \text{and} \quad \sum_{m \in \mathbb{Z}} m^0 = 1 + 2\zeta(0) = 0 . \quad (\text{C.15})$$

Similarly, we obtain the following

$$\begin{aligned} \sum_{n \in \mathbb{N}^+} \left(\sum_{m \in \mathbb{Z}} \frac{\frac{\pi^2 n^2}{L^2}}{\frac{\pi^2 n^2}{L^2} + \frac{m^2}{R^2}} \right)^2 &= \sum_{n \in \mathbb{N}^+} \left(\sum_{m \in \mathbb{Z}} \frac{\frac{m^2}{R^2}}{\frac{\pi^2 n^2}{L^2} + \frac{m^2}{R^2}} \right)^2 \\ &= \frac{(\ln q)^2}{4} \sum_{n \in \mathbb{N}} n^2 \frac{(1+q^n)^2}{(1-q^n)^2} = (\ln q)^2 \sum_{n \in \mathbb{N}} \frac{n^2 q^n}{(1-q^n)^2} = \frac{(\ln q)^2}{288} [E_4(q) - (E_2(q))^2] , \end{aligned} \quad (\text{C.16})$$

where we have used the zeta-function identity

$$\sum_{n \in \mathbb{N}} n^2 = \zeta(-2) = 0 . \quad (\text{C.17})$$

These infinite sums appear in the integral of the coincident point functions $G_{\tau\tau}$ and $G_{\sigma\sigma}$. With equations (C.14) and (C.16), we find

$$\begin{aligned} \int d\tau d\sigma G_{\tau\tau}^2 &= \int d\tau d\sigma G_{\sigma\sigma}^2 = -\frac{\pi \ln q}{576 L^2} E_4(q) , \\ \int d\tau d\sigma G_{\tau\tau} G_{\sigma\sigma} &= -\frac{\pi \ln q}{576 L^2} [E_4(q) - 2(E_2(q))^2] . \end{aligned} \quad (\text{C.18})$$

Other infinite sums appearing in the integral (C.11) include

$$\begin{aligned} \sum_{r \in \mathbb{N} + \frac{1}{2}} \sum_{m \in \mathbb{Z}} \frac{\frac{\pi^2 r^2}{L^2}}{\frac{\pi^2 r^2}{L^2} + \frac{m^2}{R^2}} &= -\frac{\ln q}{2} \sum_{r \in \mathbb{N} + \frac{1}{2}} r \frac{1+q^r}{1-q^r} = -\frac{\ln q}{48} (2E_2(q) - E_2(\sqrt{q})) , \\ \sum_{r \in \mathbb{N} + \frac{1}{2}} \sum_{m \in \mathbb{Z}} \frac{\frac{m^2}{R^2}}{\frac{\pi^2 r^2}{L^2} + \frac{m^2}{R^2}} &= -\sum_{r \in \mathbb{N} + \frac{1}{2}} \sum_{m \in \mathbb{Z}} \frac{\frac{\pi^2 r^2}{L^2}}{\frac{\pi^2 r^2}{L^2} + \frac{m^2}{R^2}} = \frac{\ln q}{48} (2E_2(q) - E_2(\sqrt{q})) , \end{aligned} \quad (\text{C.19})$$

where we have used

$$\sum_{r \in \mathbb{N} + \frac{1}{2}} r^1 = \zeta(-1, \frac{1}{2}) = \frac{1}{24} . \quad (\text{C.20})$$

Analogous to the sum in (C.16), we note

$$\begin{aligned}
\sum_{r \in \mathbb{N} + \frac{1}{2}} \left(\sum_{m \in \mathbb{Z}} \frac{\frac{\pi^2 r^2}{L^2}}{\frac{\pi^2 r^2}{L^2} + \frac{m^2}{R^2}} \right)^2 &= \sum_{r \in \mathbb{N} + \frac{1}{2}} \left(\sum_{m \in \mathbb{Z}} \frac{\frac{m^2}{R^2}}{\frac{\pi^2 r^2}{L^2} + \frac{m^2}{R^2}} \right)^2 \\
&= \frac{(\ln q)^2}{4} \sum_{r \in \mathbb{N} + \frac{1}{2}} r^2 \frac{(1+q^r)^2}{(1-q^r)^2} = (\ln q)^2 \sum_{r \in \mathbb{N} + \frac{1}{2}} \frac{r^2 q^r}{(1-q^r)^2} \\
&= \frac{(\ln q)^2}{1152} [E_4(\sqrt{q}) - 4E_4(q) - (E_2(\sqrt{q}))^2 + 4(E_2(q))^2],
\end{aligned} \tag{C.21}$$

where the zeta-function regularization reads

$$\sum_{r \in \mathbb{N} + \frac{1}{2}} r^2 = \zeta(-2, \frac{1}{2}) = 0. \tag{C.22}$$

With equations (C.19) and (C.21), we obtain the integrals of the coincident point functions $\tilde{G}_{\tau\tau}$ and $\tilde{G}_{\sigma\sigma}$:

$$\begin{aligned}
\int d\tau d\sigma \tilde{G}_{\tau\tau}^2 &= \int d\tau d\sigma \tilde{G}_{\sigma\sigma}^2 \\
&= \frac{\pi \ln q}{2304L^2} [4E_4(q) + 4E_2(\sqrt{q})E_2(q) - E_4(\sqrt{q}) - 8(E_2(q))^2], \\
\int d\tau d\sigma \tilde{G}_{\tau\tau} \tilde{G}_{\sigma\sigma} &= \frac{\pi \ln q}{2304L^2} [4E_4(q) + 2(E_2(\sqrt{q}))^2 - 4E_2(\sqrt{q})E_2(q) - E_4(\sqrt{q})].
\end{aligned} \tag{C.23}$$

Finally, we compute the following mixed terms using (C.14) and (C.19):

$$\begin{aligned}
\int d\tau d\sigma G_{\sigma\sigma} \tilde{G}_{\sigma\sigma} &= \int d\tau d\sigma G_{\tau\tau} \tilde{G}_{\tau\tau} = - \int d\tau d\sigma G_{\tau\tau} \tilde{G}_{\sigma\sigma} = - \int d\tau d\sigma G_{\sigma\sigma} \tilde{G}_{\tau\tau} \\
&= \frac{\pi}{1152L^2} \ln q [2(E_2(q))^2 - E_2(\sqrt{q})E_2(q)].
\end{aligned} \tag{C.24}$$

Next, we turn to the divergent integrals in equation (C.12). It follows from the infinite sum (C.19) that

$$\int d\tau_1 d\tau_2 (\tilde{G}_{\tau\tau}^2) \Big|_{\sigma=0} = \left(\int d\tau (\tilde{G}_{\tau\tau}) \Big|_{\sigma=0} \right)^2 = \frac{(\ln q)^2}{576L^2} (2E_2(q) - E_2(\sqrt{q}))^2. \tag{C.25}$$

For the integral on the second line of equation (C.12), we consider the infinite sum

$$\begin{aligned}
&\sum_{r, r' \in \mathbb{N} + \frac{1}{2}} \sum_{m \in \mathbb{Z}} \frac{\frac{m^4}{R^4}}{\left(\frac{\pi^2 r^2}{L^2} + \frac{m^2}{R^2} \right) \left(\frac{\pi^2 r'^2}{L^2} + \frac{m^2}{R^2} \right)} \\
&= \frac{\ln q}{2} \sum_{r, r' \in \mathbb{N} + \frac{1}{2}} \frac{1}{r^2 - r'^2} \left(r^3 \frac{1+q^r}{1-q^r} - r'^3 \frac{1+q^{r'}}{1-q^{r'}} \right) \\
&= \frac{\ln q}{2} \sum_{r \in \mathbb{N} + \frac{1}{2}} r \frac{1+q^r}{1-q^r} + \frac{(\ln q)^2}{2} \sum_{r \in \mathbb{N} + \frac{1}{2}} \frac{r^2 q^r}{(1-q^r)^2} \\
&= \frac{\ln q}{48} (2E_2(q) - E_2(\sqrt{q})) + \frac{(\ln q)^2}{2304} [E_4(\sqrt{q}) - 4E_4(q) - (E_2(\sqrt{q}))^2 + 4(E_2(q))^2],
\end{aligned} \tag{C.26}$$

where in the third line we have used the convergent sum

$$\sum_{r' \in (\mathbb{N} + \frac{1}{2}) / \{r\}} \frac{1}{r'^2 - r^2} = \frac{1}{4r^2}. \quad (\text{C.27})$$

Using equation (C.26), we find

$$\begin{aligned} \int d\tau_1 d\tau_2 (\partial_{\tau_1} \partial_{\tau_2} \tilde{G}(\tau_{12}))^2 \Big|_{\sigma_1 = \sigma_2 = 0} &= \frac{\ln q}{12L^2} (2E_2(q) - E_2(\sqrt{q})) \\ &+ \frac{(\ln q)^2}{576L^2} [E_4(\sqrt{q}) - 4E_4(q) - (E_2(\sqrt{q}))^2 + 4(E_2(q))^2]. \end{aligned} \quad (\text{C.28})$$

Finally, we consider the integrals in equation (C.13). There are three infinite sums involved in these integrals, and we start with

$$\begin{aligned} &\sum_{m_1, m_2, m_3 \in \mathbb{Z}} \sum_{r_1, r_2, r_3 \in \mathbb{N} + \frac{1}{2}} \delta_{m_1 + m_2 + m_3} \frac{\frac{m_1}{R}}{\frac{\pi^2 r_1^2}{L^2} + \frac{m_1^2}{R^2}} \frac{\frac{m_2}{R}}{\frac{\pi^2 r_2^2}{L^2} + \frac{m_2^2}{R^2}} \frac{\frac{m_3}{R}}{\frac{\pi^2 r_3^2}{L^2} + \frac{m_3^2}{R^2}} \\ &= -\frac{L^2}{16} \ln \tilde{q} \sum_{m, m' \in \mathbb{Z}} (m + m') \frac{1 - \tilde{q}^m}{1 + \tilde{q}^m} \frac{1 - \tilde{q}^{m'}}{1 + \tilde{q}^{m'}} \frac{1 - \tilde{q}^{m+m'}}{1 + \tilde{q}^{m+m'}} \\ &= -\frac{L^2}{8} \ln \tilde{q} \sum_{m, m' \in \mathbb{Z}} (m + m') \left(\frac{1}{1 - \tilde{q}^m} + \frac{1}{1 - \tilde{q}^{m'}} - \frac{1}{1 + \tilde{q}^{m+m'}} - \frac{1}{2} \right) = 0. \end{aligned} \quad (\text{C.29})$$

Using equation (C.29), we obtain the integral

$$\int d\tau_1 d\tau_2 ((\partial_{\tau_1} \tilde{G}(\tau_{12}))^2 \partial_{\tau_1} \partial_{\tau_2} \tilde{G}(\tau_{12})) \Big|_{\sigma_1 = \sigma_2 = 0} = 0. \quad (\text{C.30})$$

We also need the following infinite sum:

$$\begin{aligned} &\sum_{m_1, m_2, m_3 \in \mathbb{Z}} \sum_{n, n' \in \mathbb{N}^+} \sum_{r \in \mathbb{N} + \frac{1}{2}} \delta_{m_1 + m_2 + m_3} \frac{\frac{\pi^2 n^2}{L^2}}{\frac{\pi^2 n^2}{L^2} + \frac{m^2}{R^2}} \frac{\frac{\pi^2 n'^2}{L^2}}{\frac{\pi^2 n'^2}{L^2} + \frac{m'^2}{R^2}} \frac{1}{\frac{\pi^2 r^2}{L^2} + \frac{m^2}{R^2}} \\ &= -\frac{L^2}{16} \ln \tilde{q} \sum_{m, m' \in \mathbb{Z}} \frac{mm'}{m + m'} \frac{1 + \tilde{q}^m}{1 - \tilde{q}^m} \frac{1 + \tilde{q}^{m'}}{1 - \tilde{q}^{m'}} \frac{1 - \tilde{q}^{m+m'}}{1 + \tilde{q}^{m+m'}} \\ &= \frac{L^2}{16} \ln \tilde{q} \left[\frac{\ln \tilde{q}}{2} \sum_{m \in \mathbb{Z}} m^2 \left(\frac{1 + \tilde{q}^m}{1 - \tilde{q}^m} \right)^2 + \sum_{m \in \mathbb{Z}} m \left(\frac{4}{1 - \tilde{q}^m} - 1 \right) \right] \\ &= -\frac{L^2}{16} \ln \tilde{q} \left[\frac{2}{\ln \tilde{q}} - 4 \ln \tilde{q} \sum_{n \in \mathbb{N}^+} \frac{n^2 \tilde{q}^n}{(1 - \tilde{q}^n)^2} + \frac{1}{3} - 8 \sum_{n \in \mathbb{N}^+} \frac{n \tilde{q}^n}{1 - \tilde{q}^n} \right] \\ &= L^2 \left[\frac{(\ln \tilde{q})^2}{1152} (E_4(\tilde{q}) - (E_2(\tilde{q}))^2) - \frac{1}{8} - \frac{\ln \tilde{q}}{48} E_2(\tilde{q}) \right] = \frac{\pi^4 R^2}{288} [E_4(q) - (E_2(q))^2], \end{aligned} \quad (\text{C.31})$$

where we have used the modular transformation (A.5). Equation (C.31) simplifies the integral

$$\int d\tau_1 d\tau_2 (\tilde{G}(\tau_{12}) (\partial_{\sigma_1} \partial_{\sigma_2} G(\tau_{12}))^2) \Big|_{\sigma_1 = \sigma_2 = 0} = \frac{\pi \ln q}{144L^2} [(E_2(q))^2 - E_4(q)]. \quad (\text{C.32})$$

The last infinite sum we need is as follows

$$\begin{aligned}
& \sum_{m_1, m_2, m_3 \in \mathbb{Z}} \sum_{r, r', r'' \in \mathbb{N} + \frac{1}{2}} \delta_{m_1 + m_2 + m_3} \frac{\frac{m_1^2}{R^2}}{\frac{\pi^2 r_1^2}{L^2} + \frac{m_1^2}{R^2}} \frac{\frac{m_2^2}{R^2}}{\frac{\pi^2 r_2^2}{L^2} + \frac{m_2^2}{R^2}} \frac{1}{\frac{\pi^2 r_3^2}{L^2} + \frac{m_3^2}{R^2}} \\
&= -\frac{L^2}{16} \ln \tilde{q} \sum_{m, m' \in \mathbb{Z}} \frac{mm'}{m+m'} \frac{1-\tilde{q}^m}{1+\tilde{q}^m} \frac{1-\tilde{q}^{m'}}{1+\tilde{q}^{m'}} \frac{1-\tilde{q}^{m+m'}}{1+\tilde{q}^{m+m'}} \\
&= \frac{L^2}{16} \ln \tilde{q} \left[\frac{\ln \tilde{q}}{2} \sum_{m \in \mathbb{Z}} m^2 \left(\frac{1-\tilde{q}^m}{1+\tilde{q}^m} \right)^2 + \sum_{m \in \mathbb{Z}} m \left(\frac{4}{1+\tilde{q}^m} - 1 \right) \right] \\
&= -\frac{L^2}{16} \ln \tilde{q} \left[4 \ln \tilde{q} \sum_{n \in \mathbb{N}^+} \frac{n^2 \tilde{q}^n}{(1+\tilde{q}^n)^2} + \frac{1}{3} + 8 \sum_{n \in \mathbb{N}^+} \frac{n \tilde{q}^n}{1+\tilde{q}^n} \right] \tag{C.33} \\
&= \frac{L^2}{48} \ln \tilde{q} (E_2(\tilde{q}) - 2E_2(\tilde{q}^2)) \\
&\quad + \frac{L^2}{1152} (\ln \tilde{q})^2 [4E_4(\tilde{q}^2) + (E_2(\tilde{q}))^2 - E_4(\tilde{q}) - 4(E_2(\tilde{q}^2))^2] \\
&= \frac{\pi^4 R^2}{1152} [4(E_2(q))^2 + E_4(\sqrt{q}) - (E_2(\sqrt{q}))^2 - 4E_4(q)] .
\end{aligned}$$

Using equation (C.33), we get the integral

$$\begin{aligned}
& \int d\tau_1 d\tau_2 (\tilde{G}(\tau_{12}) (\partial_{\tau_1} \partial_{\tau_2} \tilde{G}(\tau_{12}))^2) \Big|_{\sigma_1 = \sigma_2 = 0} \\
&= \frac{\pi \ln q}{576 L^2} [(E_2(\sqrt{q}))^2 - 4(E_2(q))^2 - E_4(\sqrt{q}) + 4E_4(q)] . \tag{C.34}
\end{aligned}$$

References

- [1] Z. Komargodski and S. Zhong, *Baryon junction and string interactions*, *Phys. Rev. D* **110** (2024), no. 5 056018, [[arXiv:2405.12005](#)].
- [2] D. J. Gross and F. Wilczek, *Ultraviolet Behavior of Nonabelian Gauge Theories*, *Phys. Rev. Lett.* **30** (1973) 1343–1346.
- [3] H. D. Politzer, *Reliable Perturbative Results for Strong Interactions?*, *Phys. Rev. Lett.* **30** (1973) 1346–1349.
- [4] G. S. Bali, K. Schilling, and C. Schlichter, *Observing long color flux tubes in SU(2) lattice gauge theory*, *Phys. Rev. D* **51** (1995) 5165–5198, [[hep-lat/9409005](#)].
- [5] G. S. Bali, K. Schilling, and A. Wachter, *Complete O(v**2) corrections to the static interquark potential from SU(3) gauge theory*, *Phys. Rev. D* **56** (1997) 2566–2589, [[hep-lat/9703019](#)].
- [6] H. B. Nielsen and P. Olesen, *Vortex Line Models for Dual Strings*, *Nucl. Phys. B* **61** (1973) 45–61.
- [7] S. Mandelstam, *Vortices and Quark Confinement in Nonabelian Gauge Theories*, *Phys. Rept.* **23** (1976) 245–249.

- [8] A. A. Abrikosov, *On the Magnetic Properties of Superconductors of the Second Group*, *Sov. Phys. JETP* **5** (1957) 1174–1182.
- [9] J. S. Schwinger, *Gauge Invariance and Mass. 2.*, *Phys. Rev.* **128** (1962) 2425–2429.
- [10] A. M. Polyakov, *Quark Confinement and Topology of Gauge Groups*, *Nucl. Phys. B* **120** (1977) 429–458.
- [11] F. J. Wegner, *Duality in Generalized Ising Models and Phase Transitions Without Local Order Parameters*, *J. Math. Phys.* **12** (1971) 2259–2272.
- [12] E. H. Fradkin and S. H. Shenker, *Phase Diagrams of Lattice Gauge Theories with Higgs Fields*, *Phys. Rev. D* **19** (1979) 3682–3697.
- [13] N. Seiberg and E. Witten, *Electric - magnetic duality, monopole condensation, and confinement in $N=2$ supersymmetric Yang-Mills theory*, *Nucl. Phys. B* **426** (1994) 19–52, [[hep-th/9407087](#)]. [Erratum: *Nucl.Phys.B* 430, 485–486 (1994)].
- [14] M. Luscher and P. Weisz, *String excitation energies in $SU(N)$ gauge theories beyond the free-string approximation*, *JHEP* **07** (2004) 014, [[hep-th/0406205](#)].
- [15] O. Aharony and E. Karzbrun, *On the effective action of confining strings*, *JHEP* **06** (2009) 012, [[arXiv:0903.1927](#)].
- [16] S. Dubovsky, R. Flauger, and V. Gorbenko, *Effective String Theory Revisited*, *JHEP* **09** (2012) 044, [[arXiv:1203.1054](#)].
- [17] O. Aharony and Z. Komargodski, *The Effective Theory of Long Strings*, *JHEP* **05** (2013) 118, [[arXiv:1302.6257](#)].
- [18] Y. Nambu, *Duality and Hadrodynamics*, pp. 280–301.
- [19] T. Goto, *Relativistic quantum mechanics of one-dimensional mechanical continuum and subsidiary condition of dual resonance model*, *Prog. Theor. Phys.* **46** (1971) 1560–1569.
- [20] T. T. Takahashi, H. Matsufuru, Y. Nemoto, and H. Suganuma, *The Three quark potential in the $SU(3)$ lattice QCD*, *Phys. Rev. Lett.* **86** (2001) 18–21, [[hep-lat/0006005](#)].
- [21] T. T. Takahashi, H. Suganuma, Y. Nemoto, and H. Matsufuru, *Detailed analysis of the three quark potential in $SU(3)$ lattice QCD*, *Phys. Rev. D* **65** (2002) 114509, [[hep-lat/0204011](#)].
- [22] F. Bissey, F.-G. Cao, A. Kitson, B. G. Lasscock, D. B. Leinweber, A. I. Signal, A. G. Williams, and J. M. Zanotti, *Gluon field distribution in baryons*, *Nucl. Phys. B Proc. Suppl.* **141** (2005) 22–25, [[hep-lat/0501004](#)].
- [23] F. Bissey, F.-G. Cao, A. R. Kitson, A. I. Signal, D. B. Leinweber, B. G. Lasscock, and A. G. Williams, *Gluon flux-tube distribution and linear confinement in baryons*, *Phys. Rev. D* **76** (2007) 114512, [[hep-lat/0606016](#)].
- [24] X. Artru, *String model with baryons: Topology; classical motion*, *Nuclear Physics B* **85** (1975), no. 2 442–460.
- [25] G. C. Rossi and G. Veneziano, *A Possible Description of Baryon Dynamics in Dual and Gauge Theories*, *Nucl. Phys. B* **123** (1977) 507–545.
- [26] D. Kharzeev, *Can gluons trace baryon number?*, *Phys. Lett. B* **378** (1996) 238–246, [[nucl-th/9602027](#)].
- [27] E. Witten, *Baryons and branes in anti-de Sitter space*, *JHEP* **07** (1998) 006, [[hep-th/9805112](#)].

- [28] O. Jahn and P. de Forcrand, *Baryons and confining strings*, *Nucl. Phys. B Proc. Suppl.* **129** (2004) 700–702, [[hep-lat/0309115](#)].
- [29] Y. Imamura, *On string junctions in supersymmetric gauge theories*, *Prog. Theor. Phys.* **112** (2004) 1061–1086, [[hep-th/0410138](#)].
- [30] M. Pfeuffer, G. S. Bali, and M. Panero, *Fluctuations of the baryonic flux-tube junction from effective string theory*, *Phys. Rev. D* **79** (2009) 025022, [[arXiv:0810.1649](#)].
- [31] A. S. Bakry, X. Chen, and P.-M. Zhang, *Y-stringlike behavior of a static baryon at finite temperature*, *Phys. Rev. D* **91** (2015) 114506, [[arXiv:1412.3568](#)].
- [32] J. Altmann and P. Skands, *String junctions revisited*, *JHEP* **07** (2024) 238, [[arXiv:2404.12040](#)].
- [33] J. Polchinski and Y. Cai, *Consistency of Open Superstring Theories*, *Nucl. Phys. B* **296** (1988) 91–128.
- [34] J. L. Cardy, *Boundary Conditions, Fusion Rules and the Verlinde Formula*, *Nucl. Phys. B* **324** (1989) 581–596.
- [35] E. Witten, *Baryons in the $1/n$ Expansion*, *Nucl. Phys. B* **160** (1979) 57–115.
- [36] J. Polchinski and A. Strominger, *Effective string theory*, *Phys. Rev. Lett.* **67** (1991) 1681–1684.
- [37] J. M. Drummond, *Universal subleading spectrum of effective string theory*, [hep-th/0411017](#).
- [38] H. B. Meyer, *Poincare invariance in effective string theories*, *JHEP* **05** (2006) 066, [[hep-th/0602281](#)].
- [39] O. Aharony and N. Klinghoffer, *Corrections to Nambu-Goto energy levels from the effective string action*, *JHEP* **12** (2010) 058, [[arXiv:1008.2648](#)].
- [40] O. Aharony and M. Field, *On the effective theory of long open strings*, *JHEP* **01** (2011) 065, [[arXiv:1008.2636](#)].
- [41] O. Aharony and M. Dodelson, *Effective String Theory and Nonlinear Lorentz Invariance*, *JHEP* **02** (2012) 008, [[arXiv:1111.5758](#)].
- [42] M. Meineri, *Lorentz completion of effective string action*, *PoS ConfinementX* (2012) 041, [[arXiv:1301.3437](#)].
- [43] N. Brambilla, M. Groher, H. E. Martinez, and A. Vairo, *Effective string theory and the long-range relativistic corrections to the quark-antiquark potential*, *Phys. Rev. D* **90** (2014), no. 11 114032, [[arXiv:1407.7761](#)].
- [44] S. Hellerman, S. Maeda, J. Maltz, and I. Swanson, *Effective String Theory Simplified*, *JHEP* **09** (2014) 183, [[arXiv:1405.6197](#)].
- [45] B. B. Brandt and M. Meineri, *Effective string description of confining flux tubes*, *Int. J. Mod. Phys. A* **31** (2016), no. 22 1643001, [[arXiv:1603.06969](#)].
- [46] S. Hellerman and S. Maeda, *On Vertex Operators in Effective String Theory*, [arXiv:1701.06406](#).
- [47] J. Elias Miró, A. L. Guerrieri, A. Hebbar, J. Penedones, and P. Vieira, *Flux Tube S-matrix Bootstrap*, *Phys. Rev. Lett.* **123** (2019), no. 22 221602, [[arXiv:1906.08098](#)].
- [48] J. Elias Miró and A. Guerrieri, *Dual EFT bootstrap: QCD flux tubes*, *JHEP* **10** (2021) 126, [[arXiv:2106.07957](#)].

- [49] M. Caselle, *Effective String Description of the Confining Flux Tube at Finite Temperature*, *Universe* **7** (2021), no. 6 170, [[arXiv:2104.10486](#)].
- [50] J. Albert and A. Homrich, *Imprints of asymptotic freedom on confining strings*, [arXiv:2602.15097](#).
- [51] I. Low and A. V. Manohar, *Spontaneously broken space-time symmetries and Goldstone's theorem*, *Phys. Rev. Lett.* **88** (2002) 101602, [[hep-th/0110285](#)].
- [52] R. Auzzi, S. Bolognesi, J. Evslin, K. Konishi, and A. Yung, *NonAbelian superconductors: Vortices and confinement in $N=2$ SQCD*, *Nucl. Phys. B* **673** (2003) 187–216, [[hep-th/0307287](#)].
- [53] A. Hanany and D. Tong, *Vortex strings and four-dimensional gauge dynamics*, *JHEP* **04** (2004) 066, [[hep-th/0403158](#)].
- [54] M. Edalati and D. Tong, *Heterotic Vortex Strings*, *JHEP* **05** (2007) 005, [[hep-th/0703045](#)].
- [55] A. Athenodorou, B. Bringoltz, and M. Teper, *Closed flux tubes and their string description in $D=3+1$ $SU(N)$ gauge theories*, *JHEP* **02** (2011) 030, [[arXiv:1007.4720](#)].
- [56] A. Athenodorou, B. Bringoltz, and M. Teper, *Closed flux tubes and their string description in $D=2+1$ $SU(N)$ gauge theories*, *JHEP* **05** (2011) 042, [[arXiv:1103.5854](#)].
- [57] M. Caselle, L. Castagnini, A. Feo, F. Gliozzi, and M. Panero, *Thermodynamics of $SU(N)$ Yang-Mills theories in $2+1$ dimensions I - The confining phase*, *JHEP* **06** (2011) 142, [[arXiv:1105.0359](#)].
- [58] A. M. Polyakov, *Fine Structure of Strings*, *Nucl. Phys. B* **268** (1986) 406–412.
- [59] H. Kleinert, *The Membrane Properties of Condensing Strings*, *Phys. Lett. B* **174** (1986) 335–338.
- [60] M. Caselle, D. Fioravanti, F. Gliozzi, and R. Tateo, *Quantisation of the effective string with TBA*, *JHEP* **07** (2013) 071, [[arXiv:1305.1278](#)].
- [61] S. Dubovsky, R. Flauger, and V. Gorbenko, *Flux Tube Spectra from Approximate Integrability at Low Energies*, *J. Exp. Theor. Phys.* **120** (2015) 399–422, [[arXiv:1404.0037](#)].
- [62] C. Chen, P. Conkey, S. Dubovsky, and G. Hernández-Chifflet, *Undressing Confining Flux Tubes with $T\bar{T}$* , *Phys. Rev. D* **98** (2018), no. 11 114024, [[arXiv:1808.01339](#)].
- [63] J. F. Arvis, *The Exact $q\bar{q}$ Potential in Nambu String Theory*, *Phys. Lett. B* **127** (1983) 106–108.
- [64] P. Giudice, F. Gliozzi, and S. Lottini, *The Confining string beyond the free-string approximation in the gauge dual of percolation*, *JHEP* **03** (2009) 104, [[arXiv:0901.0748](#)].
- [65] D. M. McAvity and H. Osborn, *Conformal field theories near a boundary in general dimensions*, *Nucl. Phys. B* **455** (1995) 522–576, [[cond-mat/9505127](#)].
- [66] P. Liendo, L. Rastelli, and B. C. van Rees, *The Bootstrap Program for Boundary CFT_d* , *JHEP* **07** (2013) 113, [[arXiv:1210.4258](#)].
- [67] K. Jensen and A. O'Bannon, *Constraint on Defect and Boundary Renormalization Group Flows*, *Phys. Rev. Lett.* **116** (2016), no. 9 091601, [[arXiv:1509.02160](#)].
- [68] G. Cuomo, Z. Komargodski, and M. Mezei, *Localized magnetic field in the $O(N)$ model*, *JHEP* **02** (2022) 134, [[arXiv:2112.10634](#)].

- [69] G. Cuomo, Y.-C. He, and Z. Komargodski, *Impurities with a cusp: general theory and 3d Ising*, *JHEP* **11** (2024) 061, [[arXiv:2406.10186](#)].
- [70] A. Kapustin and M. Tikhonov, *Abelian duality, walls and boundary conditions in diverse dimensions*, *JHEP* **11** (2009) 006, [[arXiv:0904.0840](#)].
- [71] Y. Choi, C. Cordova, P.-S. Hsin, H. T. Lam, and S.-H. Shao, *Noninvertible duality defects in 3+1 dimensions*, *Phys. Rev. D* **105** (2022), no. 12 125016, [[arXiv:2111.01139](#)].
- [72] P. Niro, K. Roumpedakis, and O. Sela, *Exploring non-invertible symmetries in free theories*, *JHEP* **03** (2023) 005, [[arXiv:2209.11166](#)].
- [73] S.-H. Shao and S. Zhong, *Where non-invertible symmetries end: twist defects for electromagnetic duality*, *JHEP* **01** (2026) 118, [[arXiv:2509.21279](#)].
- [74] G. Cuomo, Z. Komargodski, and A. Raviv-Moshe, *Renormalization Group Flows on Line Defects*, *Phys. Rev. Lett.* **128** (2022), no. 2 021603, [[arXiv:2108.01117](#)].
- [75] Y. Koma and M. Koma, *Precise determination of the three-quark potential in $SU(3)$ lattice gauge theory*, *Phys. Rev. D* **95** (2017), no. 9 094513, [[arXiv:1703.06247](#)].
- [76] M. Caselle, N. Magnoli, D. Panfalone, and L. Verzichelli, *The Mass of the Baryon Junction: a lattice computation in 2 +1 dimensions*, [arXiv:2508.00608](#).
- [77] P. Lakatos and L. Losonczi, *Self-inversive polynomials whose zeros are on the unit circle*, *Publ. Math. Debrecen* **65** (2004), no. 3-4 409–420.